R & M No.3832

R &M No.3832

PROCUREMENT EXECUTIVE, MINISTRY OF DEFENCE

Aeronautical Research Council
Reports and Memoranda

THE IDENTIFICATION OF THE FLUTTER MECHANISM FROM A LARGE-ORDER FLUTTER CALCULATION

by

J.C.A. Baldock

Structures Department, RAE Farnborough, Hants

London: Her Majesty's Stationery Office
£5 NET

THE IDENTIFICATION OF THE FLUTTER MECHANISM FROM A LARGE-ORDER FLUTTER CALCULATION

By J. C. A. Baldock

Structures Department, RAE Farnborough, Hants

REPORTS AND MEMORANDA NO.3832*

February 1978

SUMMARY

The phase differences between degrees-of-freedom in a flutter calculation are discussed. From the study of phase variations with airspeed in binary systems, a technique is evolved for identifying the essential degrees-of-freedom in a large-order flutter calculation. This technique can be combined with that from a previous report in order to represent the flutter condition in a large-order flutter calculation with an equivalent two-degree-of-freedom system.

* Replaces RAE Technical Report 78017 - ARC 37871

LIST OF CONTENTS

1 INTRODUCTION

In a previous report[1] a technique was described for representing the flutter condition from a multi-degree-of-freedom system of equations by an equivalent two degree-of-freedom system. This technique involves the observation of the relative phases of the degrees-of-freedom at flutter, the division of the degrees-of-freedom into two groups with similar phases and the amalgamation of the degrees-of-freedom in each group so that a two-degree-of-freedom system is formed.

The clustering of the degrees-of-freedom into two groups has been seen to be reasonably clear in many examples, but obviously if the clustering is not clear it is difficult to apply the technique.

This Report discusses phase differences between degrees-of-freedom in a fluttering system and describes the behaviour of the phase variation with air-speed of some typical two-degree-of-freedom systems.

From the study of binary systems, a more extensive technique for condensing a large order system to two effective degrees-of-freedom is evolved. This technique is applied to a system for which the original technique was not satisfactory.

2 THE FLUTTER MECHANISM

2.1 Phase differences in a fluttering system

It is well-known[2] that a phase difference between degrees-of-freedom is related to the flow of energy into or out of a system. The background idea behind the previous report[1], which was not discussed in that report, was that the clustering of degreees-of-freedom revealed two effective degrees-of-freedom with a phase difference between them, and that this phase difference could be observed empirically and indicated the workings of the 'flutter engine', whereby the 'input energy' arising from the phase difference was overcoming the effect of 'damping actions' at flutter (using the nomenclature of Ref 2).

In order to explore more deeply the role of the phase difference, the 'energy account' for a fluttering system is found in Appendix A. For the simplest fluttering system, a two-degree-of-freedom system, the 'energy account' for the critical root or eigenvalue at flutter is, from Appendix A, equation (A-9):-

$$\left[T + V_1 + V_2\right]_0^{2\pi/\omega} = 0 = -\upsilon\pi\omega\sigma^{\frac{1}{2}}\left[b_{11}q_{10}^2 + (b_{12} + b_{21})\cos\beta\, q_{10}q_{20} + b_{22}q_{20}^2\right] - \upsilon^2\pi(c_{12} - c_{21})\sin\beta\, q_{10}q_{20} \qquad (1)$$

where $\left[T + V_1 + V_2\right]_0^{2\pi/\omega}$ is the change, in one cycle of oscillation, in the total kinetic and potential (aerodynamic and structural) energies for a particular root; equal to zero for the critical root at flutter,

q_{10}, q_{20} are the amplitudes of the degrees-of-freedom

β is the phase difference between degrees-of-freedom (positive with q_2 leading q_1)

b_{rs} are aerodynamic 'damping' coefficients in the equations of motion

c_{rs} are aerodynamic 'stiffness' coefficients in the equations of motion

υ is the equivalent airspeed parameter

σ is the atmospheric density relative to that at sea-level

ω is circular frequency.

It can be shown that the first term in (1) is always negative as long as:-

$$4b_{11}b_{22} > (b_{12} + b_{21})^2$$

which is usually satisfied.

It can be seen from (1) that, at flutter, finite values of $\sin\beta$ and $(c_{12} - c_{21})$ of the appropriate sign are needed for the 'input energy' to balance the energy dissipated by the damping forces.

In the previous report[1] it was observed that when the elements of the critical eigenvector of a large order problem, are plotted on the Argand diagram, there are often two phases around which the elements tend to cluster. This clustering seems likely to indicate two effective degrees-of-freedom and the phase angle between them. However, if the clustering is not clear, it is difficult to make more use of the generalisation of (1) for larger order systems because of the complication of the equation even for a binary. In particular β, q_{r0} and ω are implicit functions of the aerodynamic damping coefficients b_{rs} and so the apparently clear-cut distinction of aerodynamic damping coefficients in one term and aerodynamic stiffness coefficients in the other in (1) is not in fact so sharp.

A certain way of simplifying the equation for the energy account is to make the aerodynamic damping coefficients equal to zero. This simplification has some

usefulness in some aspects of the flutter problem and is often called the 'frequency coalescence' approximation because critical flutter speeds are associated then with the coalescence of two roots as the airspeed parameter υ is increased.

The nature of the 'frequency coalescence' approximation relative to the full problem is shown by Niblett[3] in his graphical representation of binary flutter.

With aerodynamic coefficients b_{rs} equal to zero, the 'energy account' at general airspeed υ for a root $(\mu + i\omega)$ is, from equation (A-8) in Appendix A for a two degree-of-freedom system:-

$$\left[T + V_1 + V_2\right]_0^{2\pi/\omega} = -\upsilon^2\left[\frac{e^{\frac{4\pi\mu}{\omega}} - 1}{4\mu}\right]\omega(c_{12} - c_{21}) \sin\beta q_{10}q_{20}$$

$$\doteq -\upsilon^2(c_{12} - c_{21}) \sin\beta q_{10}q_{20} \frac{\omega}{4\mu}\left[\left(\frac{4\pi\mu}{\omega}\right) + \tfrac{1}{2}\left(\frac{4\pi\mu}{\omega}\right)^2\right]$$

$$\doteq -\upsilon^2(c_{12} - c_{21}) \sin\beta q_{10}q_{20}\pi\left[1 + \tfrac{1}{2}\left(\frac{4\pi\mu}{\omega}\right)\right] . \qquad (2)$$

In equation (2), c_{12} and c_{21} are constant and necessarily unequal for flutter[3]. At flutter, μ is equal to zero and so $\left(\frac{4\pi\mu}{\omega}\right)$ is likely to be small for airspeeds just above the critical airspeed. The energy balance seems likely to be most dependent on $(\upsilon^2 q_{10}q_{20} \sin\beta)$. The relative significance of the terms as the airspeed is increased through the critical speed can be observed from the results of typical binary systems some of which are described in section 2.2. The solutions are without aerodynamic damping, to be consistent with (2) and also with aerodynamic damping, in order to observe how confusing the effects of aerodynamic damping may be.

2.2 Tests with binary systems

Results using some of the binary examples from Ref 3 are shown in Figs 1 to 6. On each figure the variation with airspeed of the critical frequency (proportional to the imaginary part of the root), the decay rate (proportional to the real part of the root), the phase β of degree-of-freedom 2 relative to degree-of-freedom 1 and the amplitudes q_{10} and q_{20} are shown. The degrees-of-freedom in all cases are the normal modes of the system.

2.2.1 Example 1

Example 1 is from Table 1 of Ref 3 and represents the flexure, torsion flutter of a swept wing. Fig 1 shows the results with zero aerodynamic damping. It may be seen that, at frequency coalescence at $\upsilon = 0.77$, the slopes of the decay rate and phase difference with υ show a discontinuous change and that the phase difference continues to increase as υ is increased above the critical value. The amplitude ratio q_{20}/q_{10} stays almost constant as υ increases. The phase angle, therefore, is seen to be the most distinct indicator of the flutter mechanism. Fig 2 shows the equivalent results for the critical root with aerodynamic damping coefficients appropriate to sea level (the maximum values - see Appendix A). It may be seen that for speeds above the critical speed, the phase difference and amplitude ratio are very similar to those on Fig 1 for zero aerodynamic damping. This is not unexpected as aerodynamic damping has a small effect on flutter in this case - see the variations of decay rate and frequency with airspeed in Figs 1 and 2, and also Fig 3 in Ref 3.

A point to notice is that at zero airspeed, the phase difference appears to be 90°. With normal modes as degrees-of-freedom the amplitude ratio q_{20}/q_{10} for the root shown is infinity at zero airspeed (*ie* zero q_{10} for finite q_{20}) and so the physical significance of the 90° phase angle is small. It is due to the coupling effects of aerodynamic damping - see Appendix B. However, it may confuse the comparison between the full problem and that with zero aerodynamic damping at airspeeds below the critical because the equivalent phase difference with zero aerodynamic damping is zero or 180°.

2.2.2 Example 2

Example 2 is from Table 3 of Ref 3 and represents the flutter between a wing and a free aileron carrying close to the amount of mass balance that eliminates flutter. Fig 3 shows, with zero aerodynamic damping, discontinuous changes for the slopes of the decay rate and the phase difference with υ at frequency coalescence at $\upsilon_c = 0.43$.

The amplitude ratio q_{20}/q_{10} stays almost constant above the critical airspeed. The effect of aerodynamic damping for the sea level case in this example is almost to eliminate flutter - see Fig 4 - but the phase difference and amplitude ratio above the critical airspeed are still similar to those for the zero aerodynamic damping case.

The behaviour of the phase difference in the full case as airspeed tends to zero is different from that in example 1. For example 2, with a free aileron,

section B.2 shows that the behaviour of the phase angle for the root that tends to zero as airspeed tends to zero depends on the coefficients in the equations of motion, but will often be a tendency to an angle close to 180° as in this example.

2.2.3 Example 3

Example 3 is from Table 5 of Ref 3 and represents the flutter between a wing and an aileron, the stiffness of the aileron being close to that that eliminates flutter. Fig 5 shows that with zero aerodynamic damping the minimum value of the negative decay rate is smaller than in the other examples and the flutter is much milder. Even so, the discontinuity in the slope of the phase difference at frequency coalescence is clear. Fig 6, for the sea level case shows a large effect of aerodynamic damping, the mild flutter of Fig 5 being almost eliminated. The phase difference variation with airspeed is much less marked than in Fig 5, the tendency to -90° at zero airspeed blunting the discontinuity in slope of Fig 5.

2.2.4 Conclusions from binary examples

The conclusions drawn from these binary examples are:-

(1) Even with mild flutter, the phase difference change at frequency coalescence with zero aerodynamic damping is clear.

(2) With finite aerodynamic damping, a similar change in phase difference with airspeeds above the critical can often be seen although the tendency with most systems for the phase difference to become 90° at zero airspeed may obscure the variation if the effects of aerodynamic damping on flutter are large.

(3) Phase differences in the problem with zero aerodynamic damping can assist the interpretation of the full problem with aerodynamic damping.

The conclusions from these binary examples give good pointers for the identification of the 'flutter engine' in a multi-degree-of-freedom example. In section 3, identifications are attempted from an 18 degree-of-freedom example for which the original condensation technique had not given good results.

3 MULTI-DEGREE-OF-FREEDOM EXAMPLE

3.1 Introduction

The example is concerned with the anti-symmetric flutter of a tail unit of a strike aircraft. The flutter characteristics of the tailplanes and fin were first found with an assumed rigid fuselage. A flexible fuselage was then admitted

as the first stage in complete flexible aircraft calculations. Antisymmetric flutter calculations revealed critical roots which, from the variation of real and imaginary parts with airspeed, were not obviously similar to those from the tailplane and fin fixed root calculations, and their physical bases were far from clear.

The application of the original technique and subsequent solutions that led to the modified technique are described as they were carried out. Both techniques are empirical and depend in detail on the characteristics of the system being studied. Rigorous detailed rules are hardly possible, but it is hoped that a detailed description of one example will indicate some general principles and some of the variations in approach that can be tried.

3.2 Application of the original technique for binary condensation

The fuselage and tail unit are represented by 18 degrees-of-freedom. The variation with airspeed of the seven lowest frequency roots from this system are shown in Fig 7. It may be seen that there are two reasonably hard types of flutter and one mild type, labelled A, B and C.

The critical flutter conditions for the fixed root tailplane and for the fixed root fin are $\upsilon = 0.70$, $\omega = 0.93$ and $\upsilon = 0.70$, $\omega = 0.69$ respectively. The correspondence of these points with Fig 7 is not obvious.

Recalling briefly the original technique[1], the initial equations are transformed so that normal modes are the basis of the system of the generalised coordinates, smaller order systems are found with close critical conditions (speed and frequency) to those of the complete system, and the elements of the critical eigenvectors of the smaller systems are plotted on the Argand diagram in order to see if there are two phases around which the elements tend to cluster. If two phases show up, a transformation to a two-degree-of-freedom system is made with the elements at each of the phases comprising a new generalised coordinate. The results of the application of this technique up to the plotting of the critical eigenvectors of the reduced systems are shown in Table 1 and Fig 8.

Table 1 shows the reduced systems and Fig 8 the critical eigenvectors at flutter for the critical roots of the three reduced systems. The clustering at two phases of the elements of the critical eigenvectors appears to be reasonably straightforward, and the binary transformations are shown on Fig 8. However, the binary systems derived were found not to be a good representation of all of the critical roots in Fig 7. Details are not included here. A brief description is:-

(a) Root A is reasonably represented with regard to critical speed and frequency by the binary (2 + 3) + (4 + 5 + 7) but the flutter is very mild.

(b) Root B is reasonably represented by the binary (2 + 3) + (6 + 7) with regard to the critical speed and frequency and the severity of the flutter indicated by the slope of the decay rate with airspeed at speeds above the critical.

(c) Root C is reasonably represented by the binary (1 + 2 + 4 + 7) + (5 + 6) with regard to the critical speed and frequency but the binary flutter is severe compared with the mild flutter shown on Fig 7 for the complete system.

The binary approximations are clearly not adequate; in particular because the severe flutter indicated by A on Fig 7 is not represented.

3.3 Variation of eigenvectors with airspeed

The new part of the technique is to seek additional information from the variation of eigenvectors with airspeed considering not only the full problem but also the solutions with zero aerodynamic damping.

The variations with speed of the first seven roots of the system with zero aerodynamic damping are shown on Fig 9. Comparing Fig 9 with Fig 7, it may be seen that the simple correspondences between the problems with and without aerodynamic damping in the binary examples of section 2 are not present in this multi-degree-of-freedom system with several types of flutter and it is not at all obvious which are the corresponding roots. With zero aerodynamic damping there are three types of flutter, one comparatively mild and two more severe. It can be seen from Fig 9 that one root, that marked D and F, is clearly concerned with two types of flutter, the comparatively mild type initially and then, just before the mild type of flutter reaches an upper critical speed above which the root would have been stable, another more severe type of flutter dominates. It is not clear from the variation of roots with airspeed how the three types of flutter with zero aerodynamic damping are connected with the three types of flutter in the full problem, but it seems necessary at this stage to restrict further study to the three types of flutter with zero aerodynamic damping. Any additional type of flutter in the full problem would be the result of the predominant influence of aerodynamic damping forces. The additional information to be obtained to clarify the types of flutter is the behaviour of eigenvectors with speed, which the examples of section 2 showed were complicated by aerodynamic

damping. This seems to restrict the types of flutter capable of being identified to those present with zero aerodynamic damping and modified by finite aerodynamic damping. Those essentially based on aerodynamic damping are unlikely to be clarified. It is not felt that this is a serious omission. Experience indicates that flutter based on aerodynamic damping is likely to be mild, and the graphical representation[3] indicates why this should usually be so.

The variations with speed of eigenvectors associated with the roots of interest were found. To reduce computer time, these solutions were restricted to the first seven normal modes of the system. Only small differences compared with the complete 18 degree-of-freedom system were observed in a few check computations. Comparing the variation of eigenvectors with speed for the critical roots with and without aerodynamic damping revealed the following:-

(a) the root labelled A on Fig 7 covers two types of flutter, an initial mild flutter, now called AM and then at higher airspeeds a more severe flutter, now called AMS,

(b) there are the following similarities between the types of flutter with and without aerodynamic damping:-

AM is similar to D
AMS is similar to E
B is similar to F,

(c) type C flutter with aerodynamic damping does not have an equivalent with zero aerodynamic damping.

No further attempt to identify type C is made because it is essentially due to aerodynamic damping. This is not thought to be a serious omission as the flutter speed is the highest of the three in the complete system, and the flutter is mild.

The initial comparisons of the eigenvector variations with airspeed with and without aerodynamic damping, on which the preceding conclusions are based, are not shown in this Report. They were reasonably straightforward apart from some elements in the vectors which did not show the standard pattern of the binary examples in section 2.2. These elements appeared to be associated with degrees-of-freedom that had been dropped in the degree-of-freedom dropping stage of the original technique - see Table 1 - so it seemed likely that they were playing small parts in the type of flutter being considered and that the eigenvector variations with airspeed would be clearer without them.

This suggested that the degree-of-freedom dropping procedure in the original technique still had a useful role.

The reduced systems of Table 1 were therefore solved for the variation of the critical eigenvectors with speed. Comparing these results with the corresponding results from the complete system showed:-

(a) System 23457 has a similar variation of critical eigenvector with speed as flutter AM in the complete system.

(b) System 2367 has a similar variation of critical eigenvector with speed as flutter B in the complete system.

(c) System 124567 has similar critical speed and frequency to flutter C, but the critical eigenvector variation with speed is different from that of flutter C. Also, the 124567 flutter is severe, while flutter C is mild.

Point (c) explains why the binary derived from system 124567 in the original technique did not represent flutter C - see section 3.2. This is also a warning that the reliance on the closeness of critical speeds and frequencies as criteria for the similarity of fluttering systems may prove to be confusing, and emphasises the desirability of checking the adequacy of the reduced systems for similarity with the complete system eigenvector variation with airspeed, as well as with the root variation with airspeed.

Flutter AMS could not be indicated at all by a reduced system derived from the degree-of-freedom dropping procedure. This procedure uses the critical speed and frequency of the root from the complete system as a criterion. Because flutter AMS develops from the already unstable root for flutter AM it cannot be identified by a critical speed and frequency. The eigenvectors associated with the critical eigenvalue from the system 1234567 has, therefore to be studied for flutter AMS.

Summarising, the variation of eigenvectors with airspeed with and without aerodynamic damping for the appropriate roots in the following systems are likely to show how the degrees-of-freedom are combining:-

for type AM flutter, system 23457
for type B flutter, system 2367
for type AMS flutter, system 1234567.

3.4 System 23457 for flutter type AM

The root and eigenvector variations with airspeed for the critical root with zero aerodynamic damping are shown in Fig 10. It may be seen, by comparison

with Fig 9, that the reduced system is a good representation of the complete system for υ only below 0.80. The two roots that coalesce for the critical flutter condition are shown dashed for speeds below the coalescence speed. At the critical speed $\upsilon = 0.63$, it may be seen that degrees-of-freedom 2, 3 and 7 start to rotate together relative to 4 and 5. The actual combinations of 2, 3 and 7 and of 4 and 5 are given by the amplitude ratios in Fig 10. For a completely straightforward analogy with the binary examples of section 2.3, the amplitude ratios for each combination would remain nearly constant with airspeed. Fig 10 shows that the amplitudes of degrees-of-freedom 2 and 7 have a similar ratio from $\upsilon = 0.63$ to 0.80 but 3 changes its amplitude relative to 2 and 7 and so does 5 relative to 4. This presumably reflects couplings that result in the reduced system not being a good representation for airspeeds above 0.80. However, the similarity is reasonable just above the critical airspeed 0.63, and suggests an equivalent binary could be formed by the combination of 2, 3 and 7 with 4 and 5. With this background, the system with aerodynamic damping in Fig 11 is reasonably easy to interpret. Degrees-of-freedom 2 and 3 are closely in phase at the critical speed and above, and 7 may be seen to vary with them, even though at the critical speed it is at about 90° to them. Degrees-of-freedom 4 and 5 are closely linked. The binary (2 + 3 + 7) and (4 + 5) constructed using amplitude ratios at $\upsilon = 0.60$ in Fig 11 is shown in Fig 12. Fig 12 shows that this binary represents quite well the mild onset of flutter characterising type AM in the complete system - Fig 7. It is interesting to compare this result with that derived using the original technique. The top sketch in Fig 8a gives the critical eigenvector at $\upsilon = 0.49$ and the binary transformation based on this, in which 7 was associated with 4 and 5, instead of with 2 and 3. In fact, this made little difference to the representation of the binary, presumably due to the small amplitude of 7 in this case genuinely reflecting a small effect of mode 7. The relative amplitudes cannot generally be relied upon as a measure of importance as the amplitude of an element in an eigenvector can be changed by scaling the degrees-of-freedom and does not indicate the size of the coupling terms associated with that element.

3.5 System 2367 for flutter type B

The root and eigenvector variations with airspeed for the critical root with zero aerodynamic damping are shown in Fig 13. Clearly degrees-of-freedom 2 and 3 are rotating relative to 6 and 7. The amplitude ratios are nearly constant from the coalescence speed up to $\upsilon = 1.0$.

With aerodynamic damping, the variations with airspeed are shown in Fig 14, and a similar behaviour is seen. The amplitude of 2 relative to 3 is reasonably constant, but the amplitude of 6 relative to 7 reduces a little with airspeed above the critical speed. Below the critical speed, the amplitude of 6 relative to 7 may be seen to increase considerably. This suggests that a binary with fixed relative amplitudes for 2 and 3 in one degree-of-freedom and for 6 and 7 in the other could not be a good representation over the whole range of airspeeds. The amplitude ratios chosen were those at $\upsilon = 0.70$ and the resultant binary solution is shown on Fig 15. The similarity with the full system is seen, by comparison with Fig 7, to be good over the range of airspeeds above the critical speed. Below the critical speed the full case has a higher decay rate, probably for the reason outlined above - a significant change of amplitude of degree-of-freedom 6 relative to 7 below the critical speed in the complete system.

The binary representation of flutter type B is good. A similarly good result was obtained with the original technique. Type B is a straightforward case, satisfactorily handled by either technique.

3.6 System 1234567 for flutter type AMS

Flutter type AMS is the type that could not be analysed with the original technique. Section 3.3 describes how study of the variation of the eigenvectors with airspeed for the root A in Fig 7 showed that flutter type AMS emerged out of a root already unstable in flutter type AM. A critical speed and frequency could not, therefore, be assigned to type AMS and so the degree-of-freedom dropping stage of the original technique could not be implemented as the criterion for dropping a degree-of-freedom is a small change in critical speed and frequency.

The root A from Fig 7 is reproduced on Fig 17 and, for airspeeds above 0.8, the eigenvectors that are associated with it. Below an airspeed of 0.8 the eigenvectors change to those for type AM flutter. On Fig 16, the equivalent roots and eigenvectors are shown for the case with zero aerodynamic damping. Section 3.3 describes how this root was chosen by general similarity of the eigenvector variation with airspeed with the finite aerodynamic damping case.

In Fig 16, it is reasonably clear that degrees-of-freedom 3, 4, 5, 6 and 7 are rotating relative to 1 and 2. The amplitude ratios are reasonably constant with airspeed. Fig 17 is not so clear and it would be difficult to draw firm conclusions without the information from Fig 16. Bearing in mind that at $\upsilon = 0.8$ the effect of type AM is still apparent, the behaviour about $\upsilon = 1.0$ and above is most significant. Degrees-of-freedom 4 and 5 show a similar variation with airspeed as on Fig 16 and are obviously associated. Degree-of-freedom 2 shows a

similar variation with airspeed as 4 and 5 but, comparing Figs 16 and 17, it seems likely that this is due to 2 becoming more in phase with 1 than it was in the milder flutter AM at airspeeds below 0.8. Therefore Fig 16 gives evidence that 1 and 2 are associated on Fig 17. Degrees-of-freedom 3, 6 and 7 are rather difficult to attribute on Fig 17. Their amplitudes are small, however, and, as this type of flutter is being investigated without the benefit of a smaller order system resulting from a degree-of-freedom dropping stage, it is possible that these degrees-of-freedom are not important. The binary transformation was, therefore, continued with 3, 6 and 7 associated with 4 and 5 as they are on Fig 16 but with the amplitude ratios from Fig 17 at $\upsilon = 1.0$. Above $\upsilon = 1.0$ the amplitude ratios of the important degrees-of-freedom (2 relative to 1 and 4 relative to 5) are reasonably constant. The result of the binary approximation is shown on Fig 18. Comparing Fig 18 with the complete system equivalent on Fig 7, it may be seen that the binary representation is very good, not only for the rate of change of decay rate above the critical speed around $\upsilon = 1.0$, which was the aim, but also at lower airspeeds. Comparing the binary representation for AM flutter on Fig 12 with that for AMS on Fig 18, it may be seen how similar are the critical roots of the binaries at υ about 0.5. These have been separated by the observation of the eigenvectors associated with a single root from the full case. The modified technique is obviously superior in handling this type of problem.

3.7 Types of flutter revealed

This Report is concerned with the technique rather than the detailed analysis of the example. However, it can be said that the modes involved in the binary representations of the types of flutter show that:-

(i) Type B flutter is essentially similar to the fixed root fin flutter, although fuselage flexibility modifies the lower frequency mode.

(ii) The mode shapes involved in types AM and AMS flutter all contain contributions from tailplane, fin and fuselage and it is not possible to identify clearly either fixed root fin or tailplane flutter.

4 SUMMARY OF IMPROVED TECHNIQUE

It has been shown that the study of the critical eigenvector of a large-order system as airspeed is increased through the critical airspeed can give clear indications of degrees-of-freedom to be associated in a binary representation of the complete system. The eigenvectors of the system with zero aerodynamic damping are much simpler in form and give useful additional information for interpreting the full problem.

In the example described in section 3, there is a complication in that two types of flutter are associated with a single root. This is probably an unusual effect, but the possibility complicates Stage 6 below in the summary of the procedure. The procedure is basically that of Ref 1 modified by this Report.

[Stage 0 The original solutions for roots versus airspeed for the problem with aerodynamic damping to indicate the flutter conditions to be investigated.]

Stage 1 Transform the equations so that normal modes are the basis of the generalised coordinates.

Stage 2 Find the variation of roots with airspeed for the problem with zero aerodynamic damping.

Stage 3 Find, from the system transformed to normal modes, the variation with airspeed of the eigenvectors for the critical roots for the cases with and without aerodynamic damping. (These solutions, with normal modes as degrees-of-freedom can often be with a much smaller order system than the complete system. In the example of this Report it is clear from Figs 7 and 9 that the first seven normal modes should be adequate and a few checks confirmed this.)

Stage 4 From the variation of eigenvectors with airspeed from Stage 3 find equivalent types of flutter for the cases with and without aerodynamic damping. A type of flutter with aerodynamic damping that is not similar to a type with zero aerodynamic damping is unlikely to be clarified by continuing the process for binary representation.

Stage 5 For the critical roots with aerodynamic damping, which have an equivalent in the case with zero aerodynamic damping and which are uniquely indicated by a critical speed and frequency, find by degree-of-freedom dropping the minimum system with similar critical speed and frequency.

Stage 6 For the minimum systems find the variation of the critical eigenvector with airspeed for the cases with and without aerodynamic damping and check that these are still similar to those for the complete system. Similar variations of phase angle and amplitude ratios with airspeed will indicate two sets of degrees-of-freedom to be associated. (If degree-of-freedom dropping is not possible because an already unstable root changes to a different type of

flutter, the eigenvector variation with airspeed for that different type, particularly the phases, will be complicated by unimportant modes which, however, will usually be recognised by their small amplitudes.)

Stage 7 Take the relative amplitudes within each of the two sets from the problem with aerodynamic damping just above the critical speed and form a binary transformation matrix t.

Stage 8 Transform the equations to the binary equivalent with the transformation matrix found from Stage 7, and check the binary root versus speed behaviour against that of the complete system.

Stage 9 Study the binary flutter revealed, using the mode shapes involved and the graphical representation of the binary[3].

The additional computation compared with the original technique is that required for finding the root and eigenvector variations with airspeed for the problem with zero aerodynamic damping, the eigenvector variations with airspeed for the problem with aerodynamic damping and the eigenvector variations with airspeed for critical roots of small-order systems.

Appendix A

EQUATIONS OF MOTION AND ENERGY BALANCE

A.1 Equations of motion and solutions

The equations of motion are evaluated in the form:-

$$A\ddot{q} + \sigma^{\frac{1}{2}}\upsilon B\dot{q} + (\upsilon^2 C + E)q = 0 \qquad (A\text{-}1)$$

where q is a column matrix of generalised coordinates

υ is an airspeed parameter proportional to equivalent airspeed

σ is atmospheric density relative to sea level

A is a square matrix of structural inertia coefficients

B is a square matrix of aerodynamic damping coefficients

C is a square matrix of aerodynamic stiffness coefficients

E is a square matrix of structural stiffness coefficients.

Note At constant equivalent airspeed, the aerodynamic damping forces will be relatively larger the lower the altitude.

The aerodynamic matrices B and C are functions of Mach number M and frequency parameter ν, and the elements of the matrix are evaluated with an assumption of simple harmonic motion. If constant values of M and ν are assumed, then matrices B and C are constant.

Solutions to (A-1) are obtained by:-

(a) assuming constant values for M and $\sigma^{\frac{1}{2}}$, *ie* constant values for Mach number and altitude,

(b) assuming a constant value for frequency parameter ν,

(c) introducing specific values of υ and solving the resulting equations with constant coefficients for roots which are generally complex.

Critical flutter conditions are indicated at interpolated values of airspeed υ that result in pure imaginary roots. The interpolated airspeed and frequency imply a derived frequency parameter. Solutions are repeated with aerodynamic matrices B and C for several (not usually more than three) values of frequency parameter, and critical flutter conditions with assumed frequency parameter consistent with derived frequency parameter obtained by interpolation.

The assumption of simple harmonic motion made in the evaluation of the aerodynamic matrices B and C is satisfied at flutter but not generally. However, experience indicates that this inconsistency seldom leads to confusing

results and the approximation is certainly adequate to indicate whether the flutter is mild or severe.

The lining up of assumed and derived frequency parameter can be omitted when the effect of changing structural parameters on flutter speed is being found. These studies can be made with a single set of aerodynamic data with a frequency parameter close, within ±30%, say, of the frequency parameters of the flutter conditions.

The effect of Mach number and altitude are found independently and no attempt is made until a very late stage in an investigation to obtain values of critical equivalent airspeed, Mach number and altitude consistent with the standard atmosphere.

It is considered that time and computation effort are better spent in trying to understand the flutter mechanisms inherent in equation (A-1) with constant coefficients than in ensuring consistencies in often unimportant parameters. The form of (A-1) is preferred as it emphasises the role of the dominant parameter in flutter, equivalent airspeed.

A.2 The energy account

Following Appendix III of Ref 2, with equations of motion (A-1) together with external generalised forces Q :-

$$A\ddot{q} + \sigma^{\frac{1}{2}}\upsilon B\dot{q} + (\upsilon^2 C + E)q = Q \ .$$

The rate of work being done on the system by Q can be written:-

$$\dot{q}^T Q \equiv \dot{q}^T [A\ddot{q} + \sigma^{\frac{1}{2}}\upsilon B\dot{q} + (\upsilon^2 C + E)q]$$

where accent T denotes the transpose of a matrix.
For a free system Q is zero, and so the 'energy account' for a free system can be written:-

$$\dot{q}^T [A\ddot{q} + \sigma^{\frac{1}{2}}\upsilon B\dot{q} + (\upsilon^2 C + E)q] = 0 \ . \qquad (A\text{-}2)$$

The kinetic energy of the system T can be written:-

$$2T = \dot{q}^T A\dot{q}$$

therefore $$\frac{dT}{dt} = \tfrac{1}{2}[\dot{q}^T A\ddot{q} + \ddot{q}^T A\dot{q}]$$

and the scalar quantities are equal to their transposes

therefore $$\frac{dT}{dt} = \tfrac{1}{2}[\dot{q}^T A\ddot{q} + \dot{q}^T A^T\ddot{q}]$$

$$= \tfrac{1}{2}\dot{q}^T(A + A^T)\ddot{q} \equiv \dot{q}^T A\ddot{q} \qquad \text{(A-3)}$$

since A is symmetric.

The potential energy associated with the symmetric part of the aerodynamic stiffness terms C can be written:-

$$2V_1 = \upsilon^2 q^T\left(\frac{C + C^T}{2}\right)q$$

therefore $$\frac{dV_1}{dt} = \frac{\upsilon^2}{2}\left[q^T\left(\frac{C + C^T}{2}\right)\dot{q} + \dot{q}^T\left(\frac{C + C^T}{2}\right)q\right]$$

$$= \frac{\upsilon^2}{2}\left[\dot{q}^T\left(\frac{C^T + C}{2}\right)q + \dot{q}^T\left(\frac{C + C^T}{2}\right)q\right]$$

$$= \upsilon^2\dot{q}^T\left(\frac{C + C^T}{2}\right)q \quad . \qquad \text{(A-4)}$$

The potential energy associated with the structural stiffness terms E can be written:-

$$2V_2 = q^T Eq$$

therefore $$\frac{dV_2}{dt} = \tfrac{1}{2}[q^T E\dot{q} + \dot{q}^T Eq]$$

$$= \tfrac{1}{2}[\dot{q}^T E^T q + \dot{q}^T Eq]$$

$$= \tfrac{1}{2}\dot{q}^T(E^T + E)q \equiv \dot{q}^T Eq \qquad \text{(A-5)}$$

since E is symmetric.

A dissipation function F can be written:-

$$2F = \sigma^{\frac{1}{2}} v \dot{q}^T B \dot{q} \quad . \tag{A-6}$$

Using (A-3), (A-4), (A-5) and (A-6), the energy account (A-2) can be written:-

$$\frac{d(T + V_1 + V_2)}{dt} = - 2F - v^2 \dot{q}^T \left(\frac{C - C_T}{2} \right) q \quad . \tag{A-7}$$

If (A-7) is integrated, for a two degree-of-freedom system, over the period $t = 2\pi/\omega$ of a motion:-

$$q \equiv e^{\mu t} \begin{bmatrix} q_{10} \sin \omega t \\ q_{20} \sin(\omega t + \beta) \end{bmatrix} ,$$

it can be shown that:-

$$\left[T + V_1 + V_2 \right]_0^{2\pi/\omega} =$$

$$- \sigma^{\frac{1}{2}} v \left[\frac{e^{\frac{4\pi\mu}{\omega}} - 1}{4\mu} \right] \left[\omega^2 b_{11} q_{10}^2 + \omega(b_{12} + b_{21})(\mu \sin \beta + \omega \cos \beta) q_{10} q_{20} \right.$$

$$\left. + b_{22}(\mu^2 + \omega^2 + \mu\omega \sin 2\beta - \mu^2 \cos 2\beta) q_{20}^2 \right]$$

$$- v^2 \left[\frac{e^{\frac{4\pi\mu}{\omega}} - 1}{4\mu} \right] \left[\omega(c_{12} - c_{21}) \sin \beta \, q_{10} q_{20} \right] \quad . \tag{A-8}$$

It can be shown that the first expression in (A-8) is negative for all values of q_{10}, q_{20}, ω, μ and β if:-

$$b_{11} > 0$$

$$4 b_{11} b_{22} > (b_{12} + b_{21})^2 \quad .$$

This condition is usually satisfied - an exception indicates a susceptibility to single degree-of-freedom flutter. Usually, therefore, the energy of the system

over one cycle is reduced by one of the actions of the aerodynamic damping coefficients b_{rs}, and whether it increases, stays constant or reduces depends on the sign and magnitude of the second expression in (8-A), *ie* on:-

$$- \upsilon^2 \left[\frac{4\pi\mu}{\frac{\omega}{e} - 1} \right] \left[\omega(c_{12} - c_{21}) \sin\beta \, q_{10} q_{20} \right] .$$

It can be shown that:-

$$\left[\frac{4\pi\mu}{\frac{\omega}{e} - 1} \right] > 0$$

for all values of μ .

An important feature in the energy account is therefore seen to be the sign of:-

$$(c_{12} - c_{21}) \sin\beta .$$

At flutter μ is equal to zero, and (A-8) simplifies to:-

$$\left[T + V_1 + V_2 \right]_0^{2\pi/\omega} = - \sigma^{\frac{1}{2}} \upsilon\pi\omega \left[b_{11} q_{10}^2 + (b_{12} + b_{21}) \cos\beta \, q_{10} q_{20} + b_{22} q_{20}^2 \right]$$

$$- \upsilon^2 \pi (c_{12} - c_{21}) \sin\beta \, q_{10} q_{20} . \qquad \text{(A-9)}$$

Appendix B

THE FORM OF EIGENVECTORS AT SMALL AIRSPEEDS

B.1 We consider binary equations in which normal modes are the generalised coordinates:-

$$\left[\begin{array}{c|c} a_{11}\lambda^2 + \sigma^{\frac{1}{2}}\upsilon b_{11}\lambda + \upsilon^2 c_{11} + e_{11} & \sigma^{\frac{1}{2}}\upsilon b_{12}\lambda + \upsilon^2 c_{12} \\ \hline \sigma^{\frac{1}{2}}\upsilon b_{21}\lambda + \upsilon^2 c_{21} & a_{22}\lambda^2 + \sigma^{\frac{1}{2}}\upsilon b_{22}\lambda + \upsilon^2 c_{22} + e_{22} \end{array}\right] \left[\begin{array}{c} q_1 \\ -- \\ q_2 \end{array}\right] = 0 \; . \qquad \ldots\ldots \quad (B\text{-}1)$$

For small airspeed υ ,

$$\upsilon^2 \ll \upsilon$$

and the equations are approximately:-

$$\left[\begin{array}{c|c} a_{11}\lambda^2 + \sigma^{\frac{1}{2}}\upsilon b_{11}\lambda + e_{11} & \sigma^{\frac{1}{2}}\upsilon b_{12}\lambda \\ \hline \sigma^{\frac{1}{2}}\upsilon b_{21}\lambda & a_{22}\lambda^2 + \sigma^{\frac{1}{2}}\upsilon b_{22}\lambda + e_{22} \end{array}\right] \left[\begin{array}{c} q_1 \\ -- \\ q_2 \end{array}\right] = 0 \; . \qquad \ldots\ldots \quad (B\text{-}2)$$

The roots are found by evaluating the determinant of the matrix of coefficients and solving the polynomial in λ . The roots are approximately:-

$$\lambda = -\sigma^{\frac{1}{2}}\frac{\upsilon}{2}\frac{b_{11}}{a_{11}} \pm i\left(\frac{e_{11}}{a_{11}}\right)^2 \; , \quad -\sigma^{\frac{1}{2}}\frac{\upsilon}{2}\frac{b_{22}}{a_{22}} \pm i\left(\frac{e_{22}}{a_{22}}\right)^{\frac{1}{2}} \; . \qquad (B\text{-}3)$$

The amplitude ratio q_2/q_1 is given by:-

$$\frac{q_2}{q_1} = \frac{-\sigma^{\frac{1}{2}}\upsilon b_{21}\lambda}{a_{22}\lambda^2 + \sigma^{\frac{1}{2}}\upsilon b_{22}\lambda + e_{22}} \; . \qquad (B\text{-}4)$$

Evaluating this for the root $\lambda = -\frac{\sigma^{\frac{1}{2}}\upsilon b_{11}}{2a_{11}} + i\left(\frac{e_{11}}{a_{11}}\right)^{\frac{1}{2}}$ *ie* finding the amplitude ratio of the 2nd coordinate relative to that of the 1st coodinate for the root closest to that for the 1st coordinate as a single degree-of-freedom,

$$\frac{q_2}{q_1} \doteq \frac{-\sigma^{\frac{1}{2}}\upsilon b_{21}\left[-\frac{\sigma^{\frac{1}{2}}\upsilon b_{11}}{2a_{11}}+i\left(\frac{e_{11}}{a_{11}}\right)^{\frac{1}{2}}\right]}{\left[-\frac{e_{11}}{a_{11}}-\frac{i\sigma^{\frac{1}{2}}\upsilon b_{11}}{a_{11}}\left(\frac{e_{11}}{a_{11}}\right)^{\frac{1}{2}}\right]a_{22}+\left[-\frac{\sigma^{\frac{1}{2}}\upsilon b_{11}}{2a_{11}}+i\left(\frac{e_{11}}{a_{11}}\right)^{\frac{1}{2}}\right]\sigma^{\frac{1}{2}}\upsilon b_{22}+e_{22}}$$

$$\doteq \frac{\left[-i\sigma^{\frac{1}{2}}\upsilon b_{21}\left(\frac{e_{11}}{a_{11}}\right)^{\frac{1}{2}}\right]}{\left[-\frac{e_{11}a_{22}}{a_{11}}+e_{22}\right]+i\sigma^{\frac{1}{2}}\upsilon\left(\frac{e_{11}}{a_{11}}\right)^{\frac{1}{2}}\left[-\frac{b_{11}a_{22}}{a_{11}}+b_{22}\right]} \text{ neglecting } \upsilon^2 \ . \tag{B-5}$$

As υ tends to zero, the denominator tends to:-

$$\left[-\frac{e_{11}a_{22}}{a_{11}}+e_{22}\right]$$

and so q_2/q_1 tends to:

$$\alpha\left[-i\sigma^{\frac{1}{2}}\upsilon b_{21}\left(\frac{e_{11}}{a_{11}}\right)^{\frac{1}{2}}\right] \tag{B-6}$$

where α is real and finite.

If q_2/q_1 is computed for small υ, this corresponds to a phase $\pm 90^{\circ}$.

B.2 If one of the structural stiffnesses is zero, the behaviour as υ tends to zero is different for the root that tends to zero as υ tends to zero. Then, for small υ with $e_{22} = 0$, (B-3) is replaced by:-

$$\lambda \doteq \frac{\sigma^{\frac{1}{2}}\upsilon b_{22}}{2a_{22}}+i\upsilon\left(\frac{c_{22}}{a_{22}}-\frac{\sigma b_{22}^2}{4a_{22}^2}\right)^{\frac{1}{2}} \tag{B-7}$$

and, neglecting υ^2 in the numerator,

$$\frac{q_2}{q_1} \doteq \frac{e_{11}}{-\sigma^{\frac{1}{2}}\upsilon b_{12}\left[\frac{\sigma^{\frac{1}{2}}\upsilon b_{22}}{2a_{22}} + i\upsilon\left(\frac{c_{22}}{a_{22}} - \frac{\sigma b_{22}^2}{4a_{22}^2}\right)^{\frac{1}{2}}\right] - \upsilon^2 c_{12}},$$

$$\doteq \frac{e_{11}}{-\upsilon^2\left(\frac{\sigma b_{12} b_{22}}{2a_{22}} + c_{12}\right) - i\upsilon^2\sigma^{\frac{1}{2}} b_{12}\left(\frac{c_{22}}{a_{22}} - \frac{\sigma b_{22}^2}{4a_{22}^2}\right)^{\frac{1}{2}}}. \qquad \text{(B-8)}$$

Therefore, as υ tends to zero, q_2/q_1 tends to infinity but, in general, to a 'complex' infinity. For many flutter systems, including that shown in Fig 4, c_{12} is much greater than b_{12}. In that case q_2/q_1 would tend to a nearly 'real' infinity, and, if q_2/q_1 is computed for small υ, this corresponds to a phase close to zero or 180°.

Table 1

APPLICATION TO EXAMPLE OF ORIGINAL TECHNIQUE

Label	18 modes		Modes remaining after degree-of-freedom dropping			Deduced binary
	υ_c	ω_c	Modes	υ_c	ω_c	
A	0.50	0.58	2-3-4-5-7	0.51	0.58	(2 + 3) + (4 + 5 + 7)
B	0.69	0.78	2-3-6-7	0.72	0.78	(2 + 3) + (6 + 7)
C	0.80	0.61	1-2-4-5-6-7	0.80	0.62	(1 + 2 + 4 + 7) + (5 + 6)

LIST OF SYMBOLS

A	matrix of structural inertia coefficients
a_{rs}	typical element of A
B	matrix of aerodynamic damping coefficients
C	matrix of aerodynamic stiffness coefficients
E	matrix of structural stiffness coefficients
F	dissipation function - see Appendix A
M	Mach number
Q_r	generalised force r
q_r	generalised coordinate r
q_{r0}	the amplitude of generalised coordinate r
T	kinetic energy
t	transformation matrix in Fig 8
V	total structural and aerodynamic potential energy
$\left[T + V\right]_0^{2\pi/\omega}$	see equations (1) and (A-10)
β	phase angle
λ	complex root $\mu \pm i\omega$
μ	real part of root
ν	frequency parameter
σ	atmospheric density relative to sea level
υ	equivalent airspeed
υ_c	critical flutter value of υ
ω	imaginary part of root proportional to frequency
ω_c	critical flutter value of ω
$n_{\frac{1}{2}}$	cycles to half amplitude
accent T	denotes the transpose of a matrix

REFERENCES

No.	Author	Title, etc
1	J.C.A. Baldock	A technique for analysing the results of a flutter calculation. ARC R & M No.3765 (1975)
2	W.J. Duncan	The fundamentals of flutter. ARC R & M No.2417 (1951)
3	Ll.T. Niblett	A graphical representation of the binary flutter equations in normal coordinates. ARC R & M No.3496 (1968)

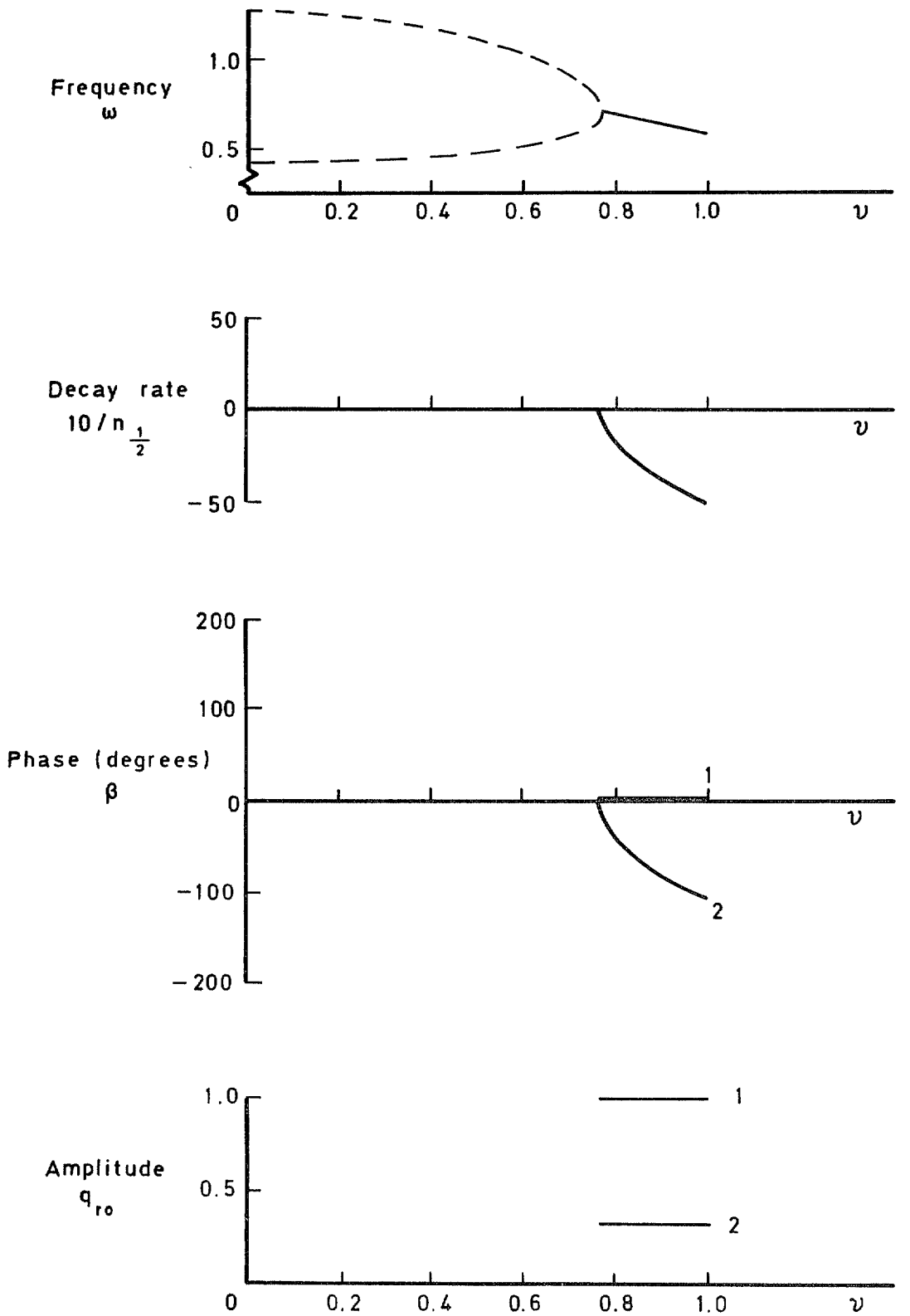

Fig 1 Binary example 1 — zero aero damping

Fig 2

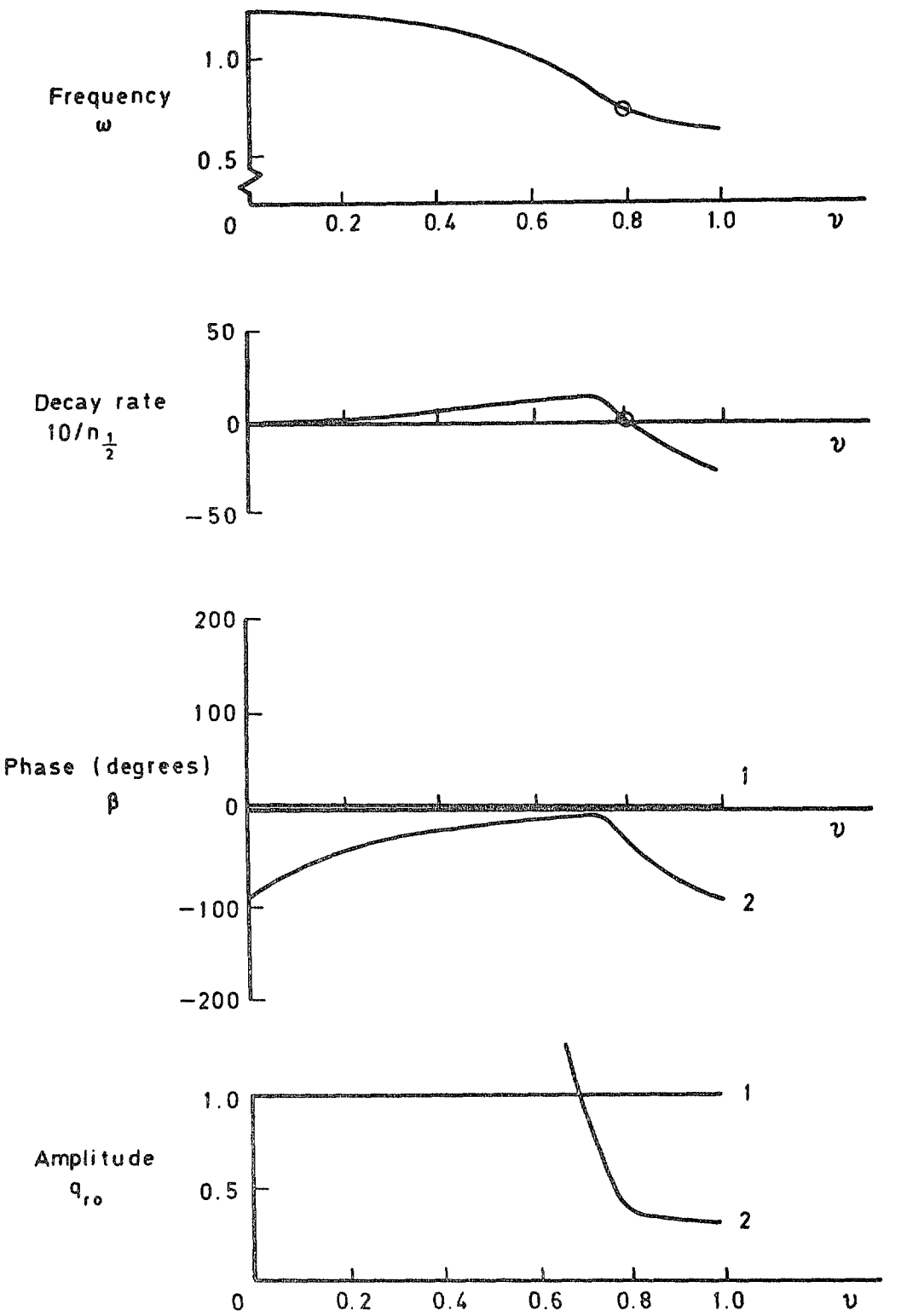

Fig 2 Binary example 1 — sea level aero damping

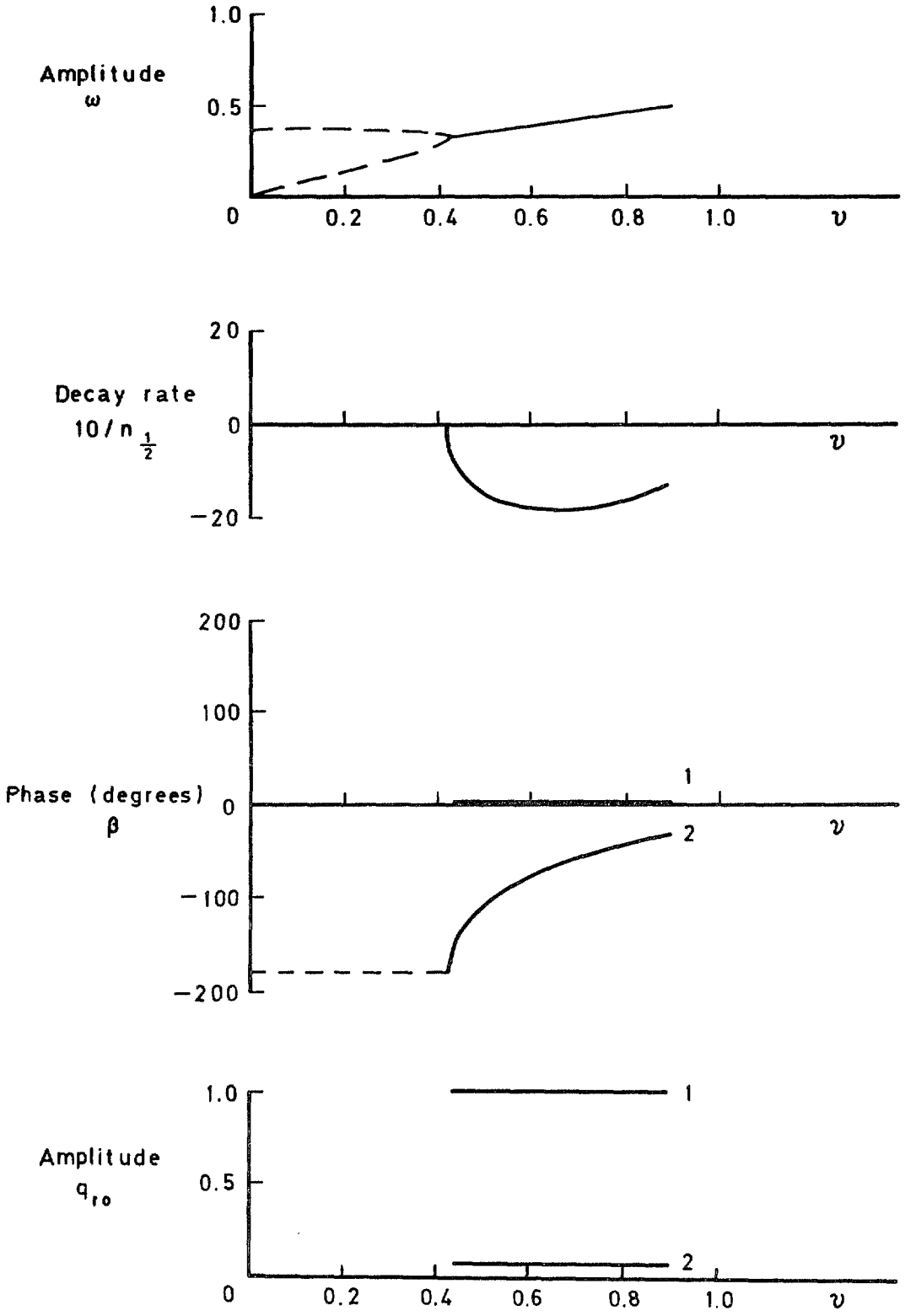

Fig 3 Binary example 2 — zero aero damping

Fig 4

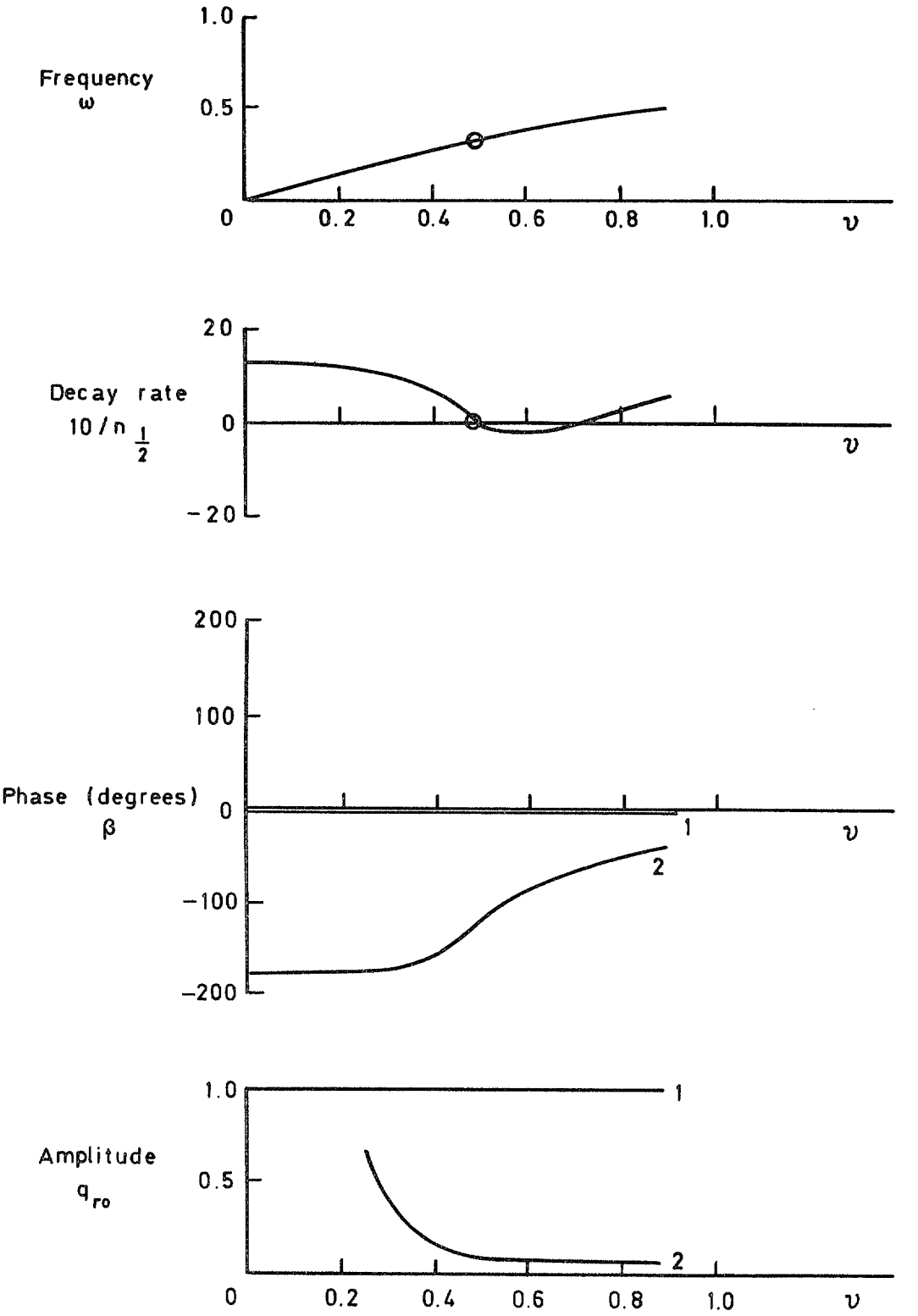

Fig 4 Binary example 2 — sea level aero damping

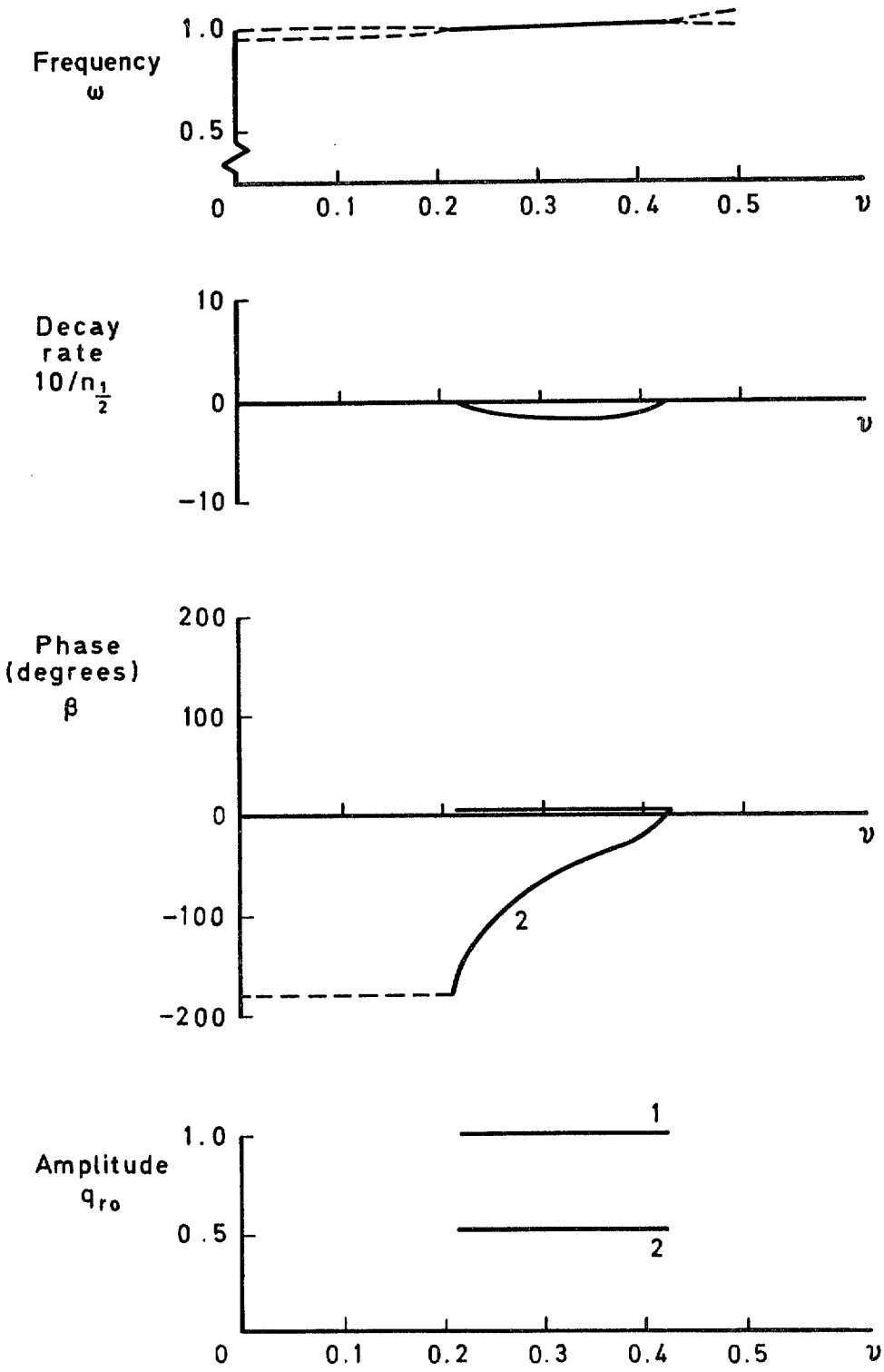

Fig 5 Binary example 3 — zero aero damping

Fig 6

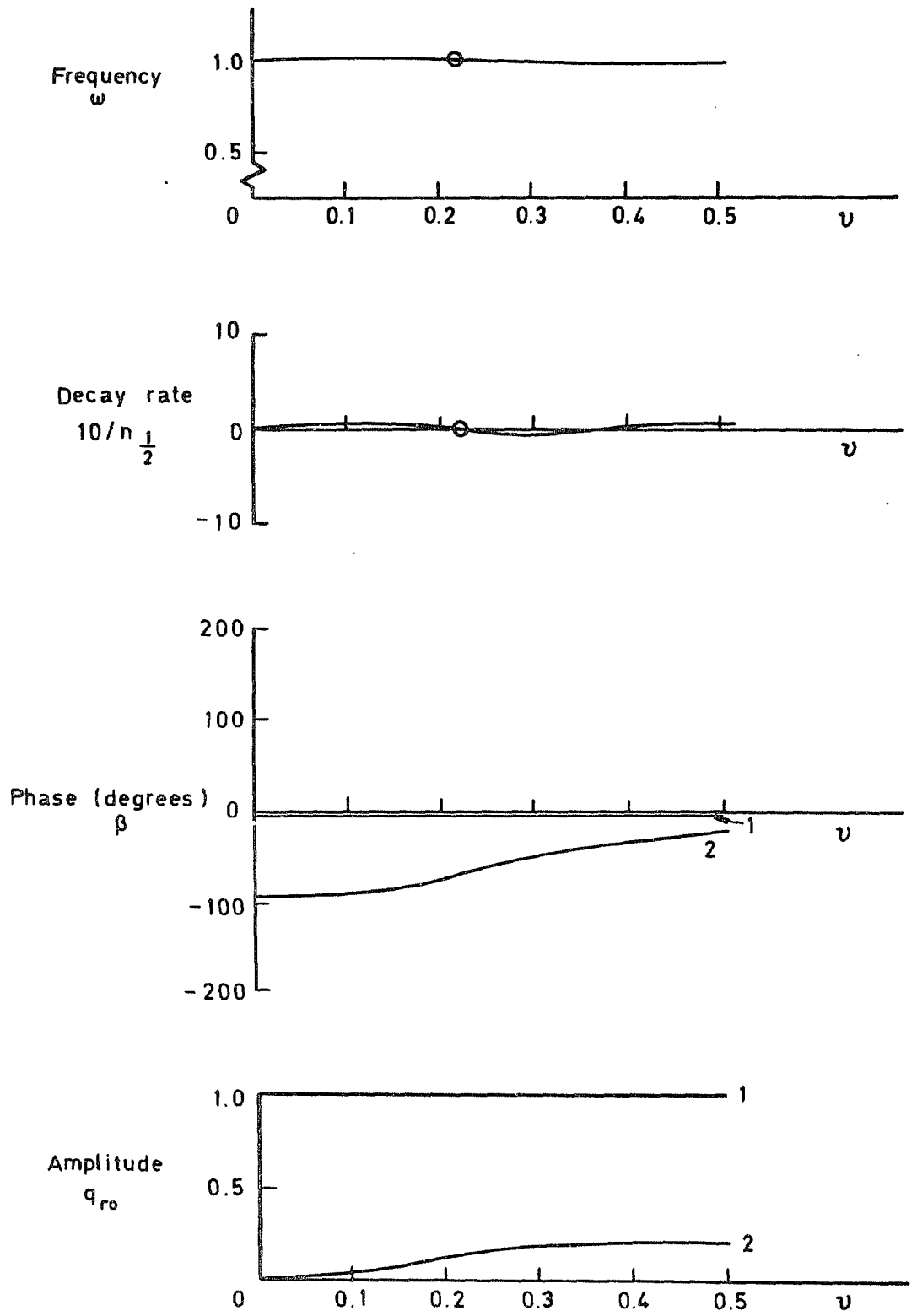

Fig 6 Binary example 3 — sea level aero damping

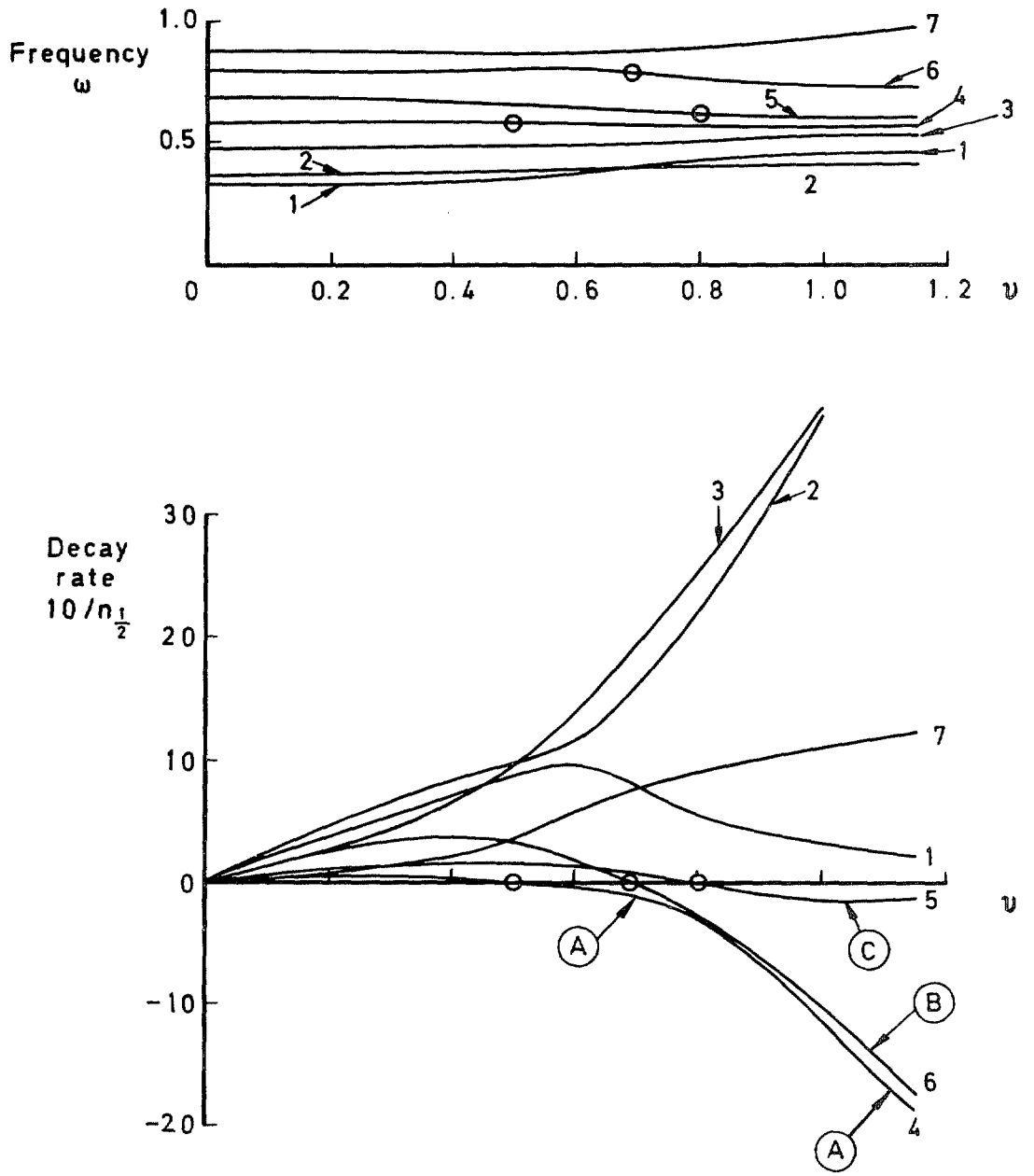

Fig 7 Results from 18 degree-of-freedom system — sea level aero damping

Fig 8

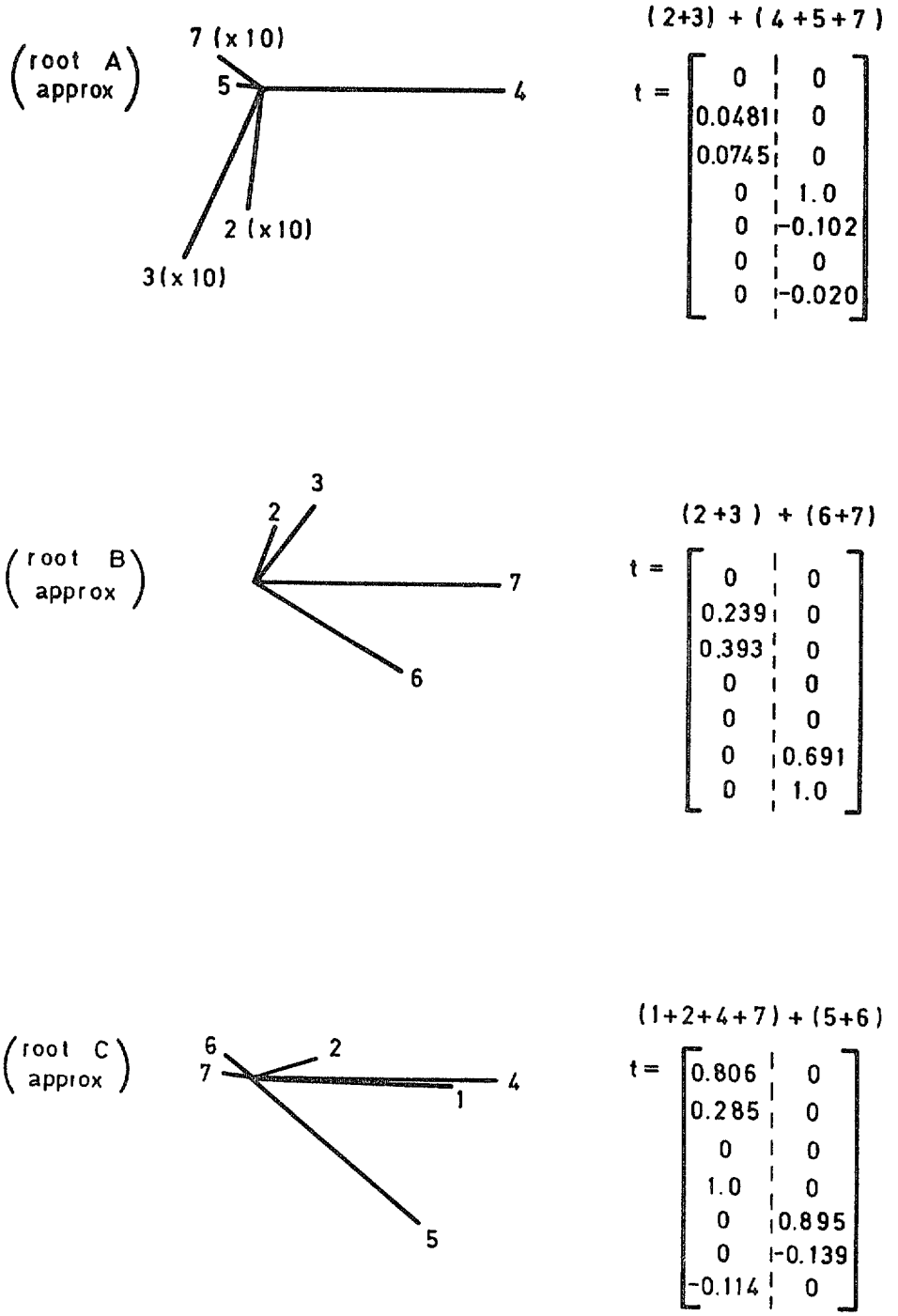

Fig 8 Critical eigenvectors at flutter

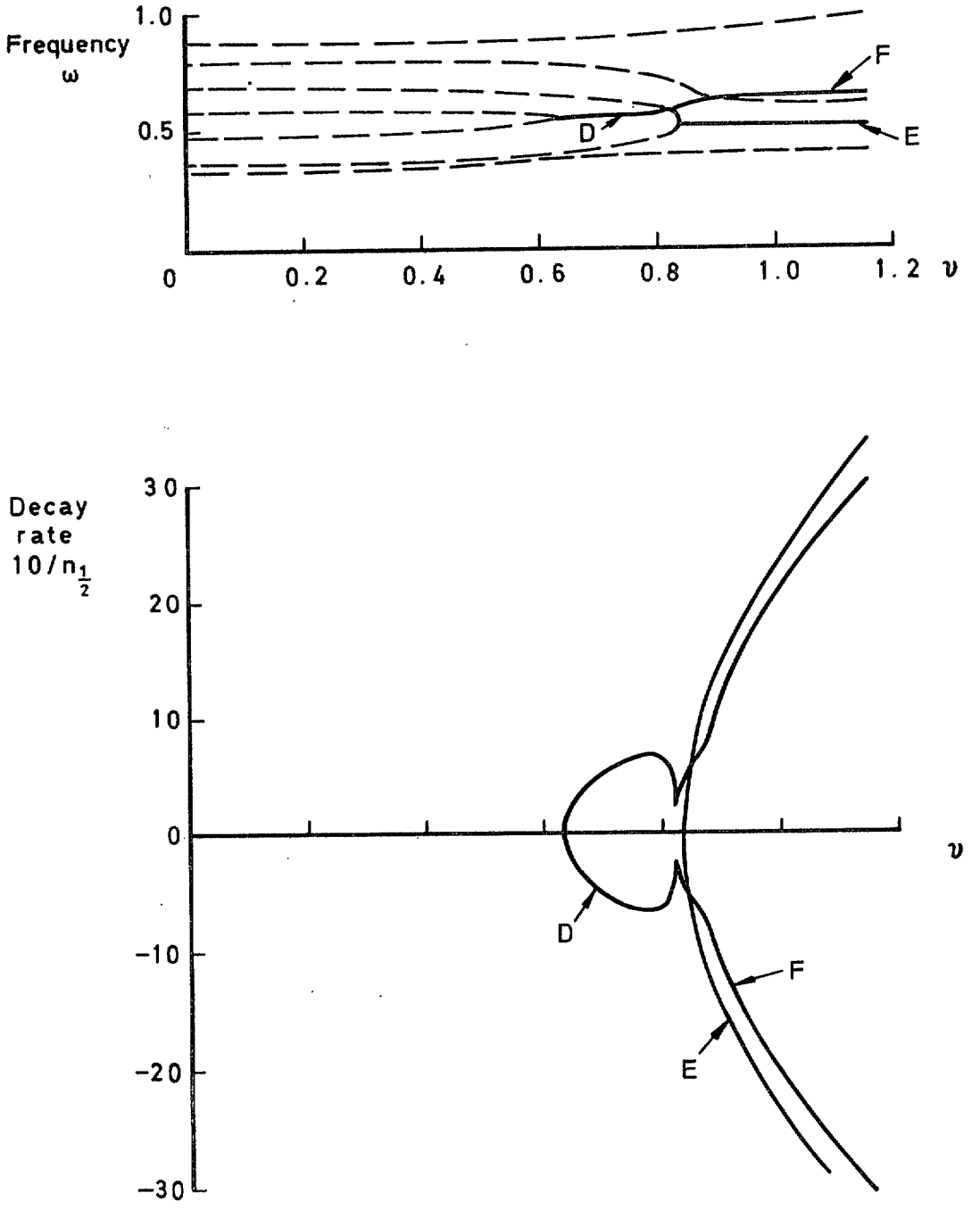

Fig 9 Results from 18 degree-of-freedom system — zero aero damping

Fig 10

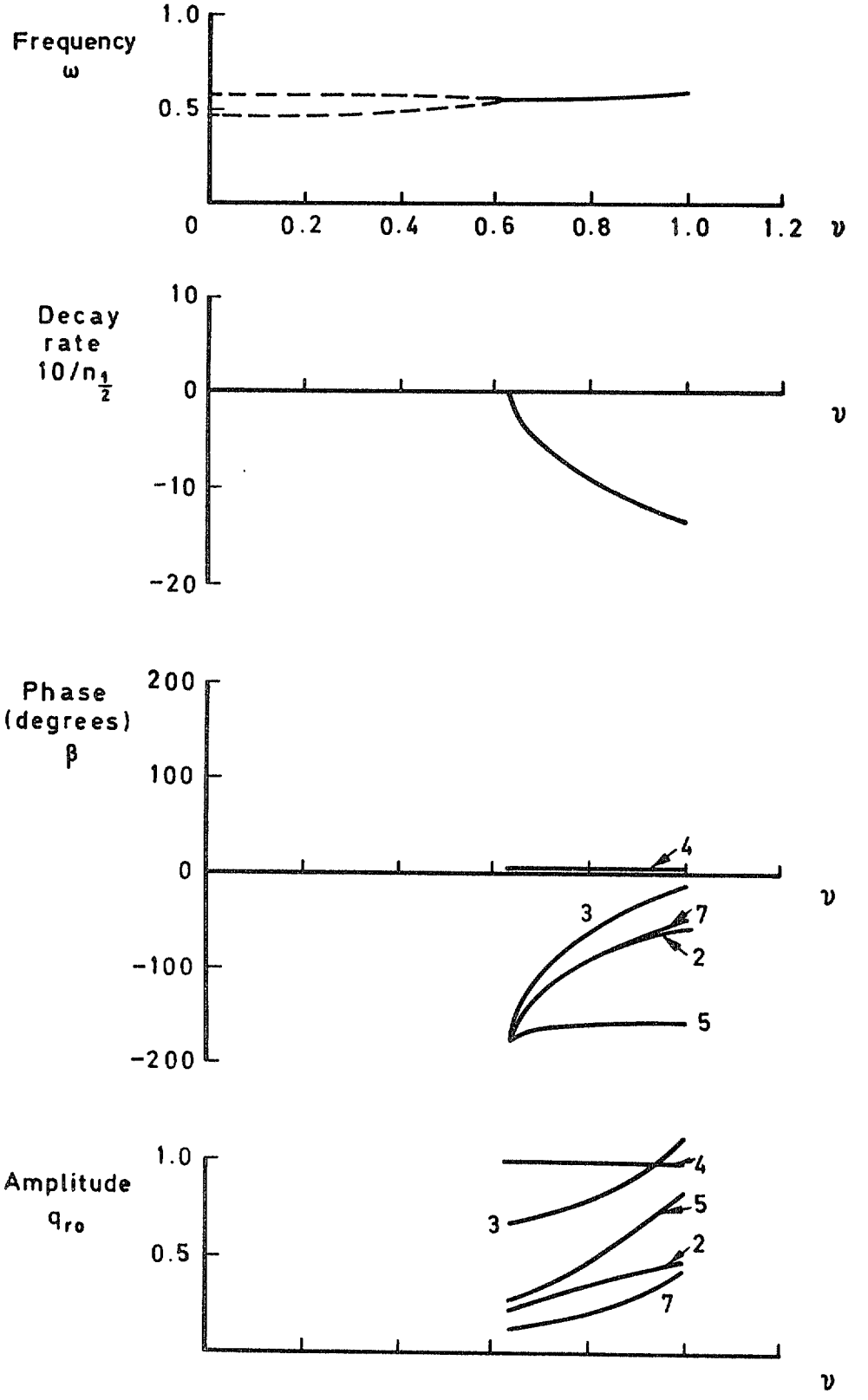

Fig 10 Critical root and eigenvector variation with airspeed — system 23457 — zero aero damping

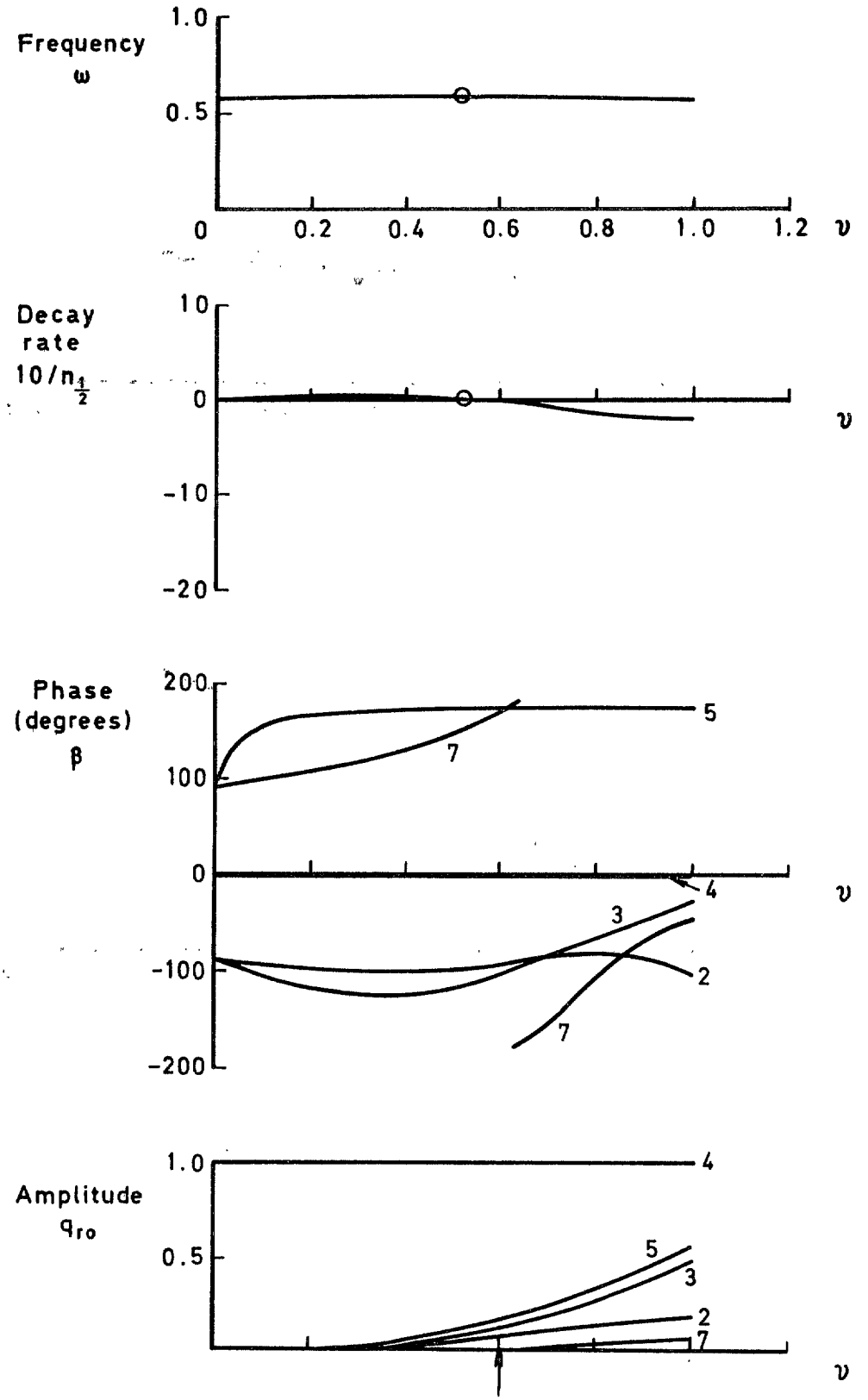

Fig 11 Critical root and eigenvector variation with airspeed — system 23457 — sea level aero damping

Fig 12

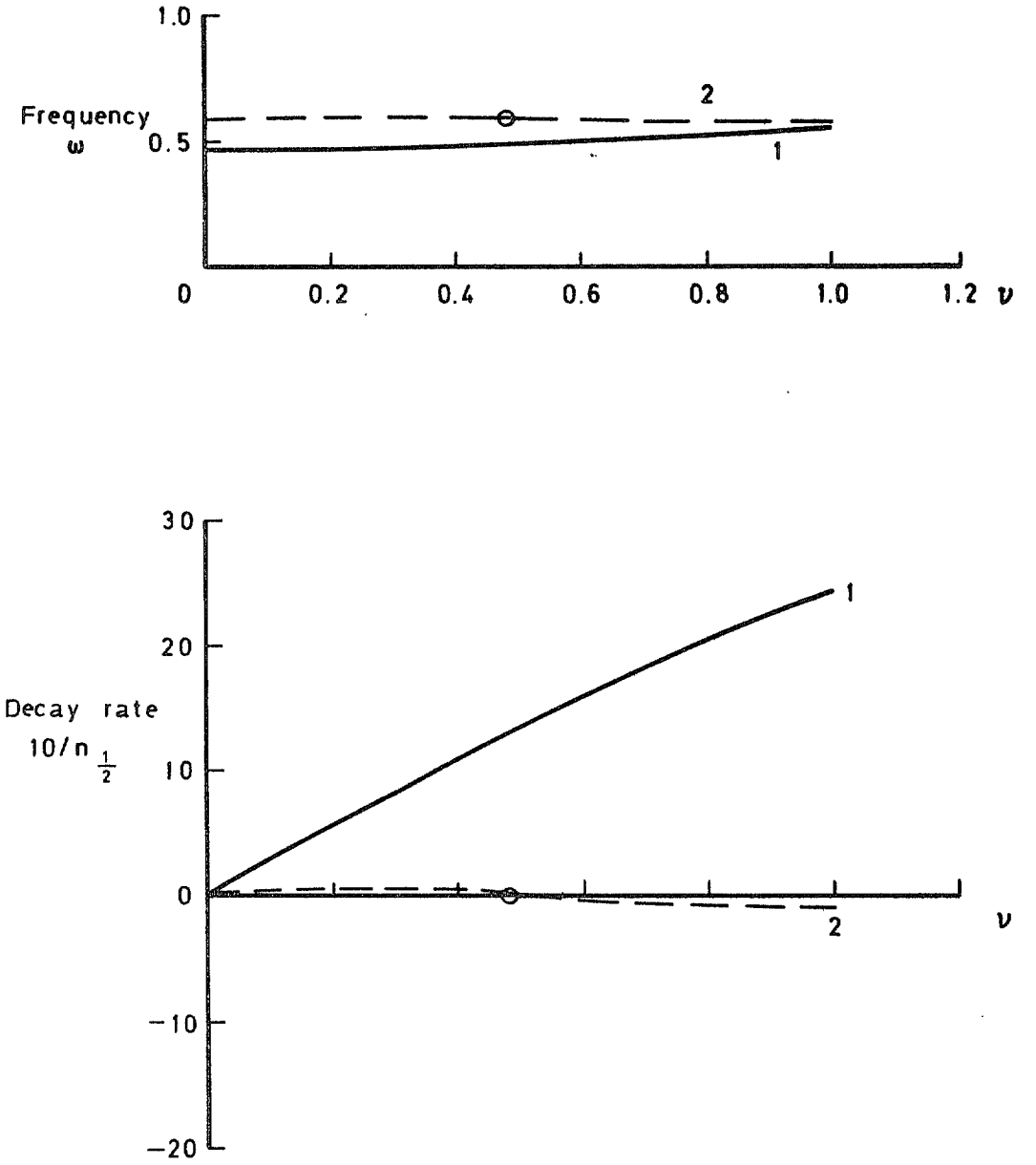

Fig 12 Binary equivalent for flutter type AM (2 + 3 + 7) + (4 + 5)

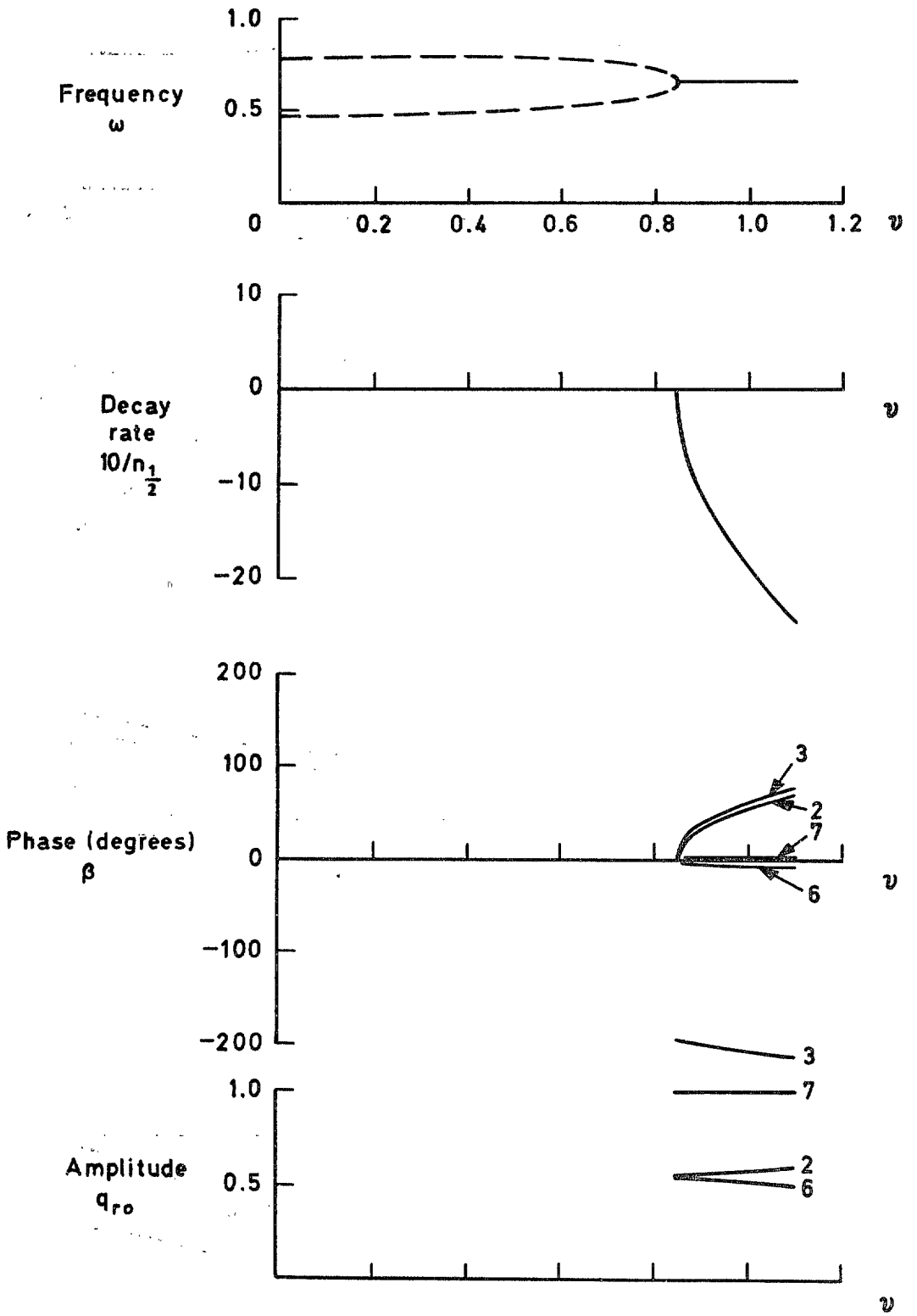

Fig 13 Critical root and eigenvector variation with airspeed — system 2367 — zero aero damping

Fig 14

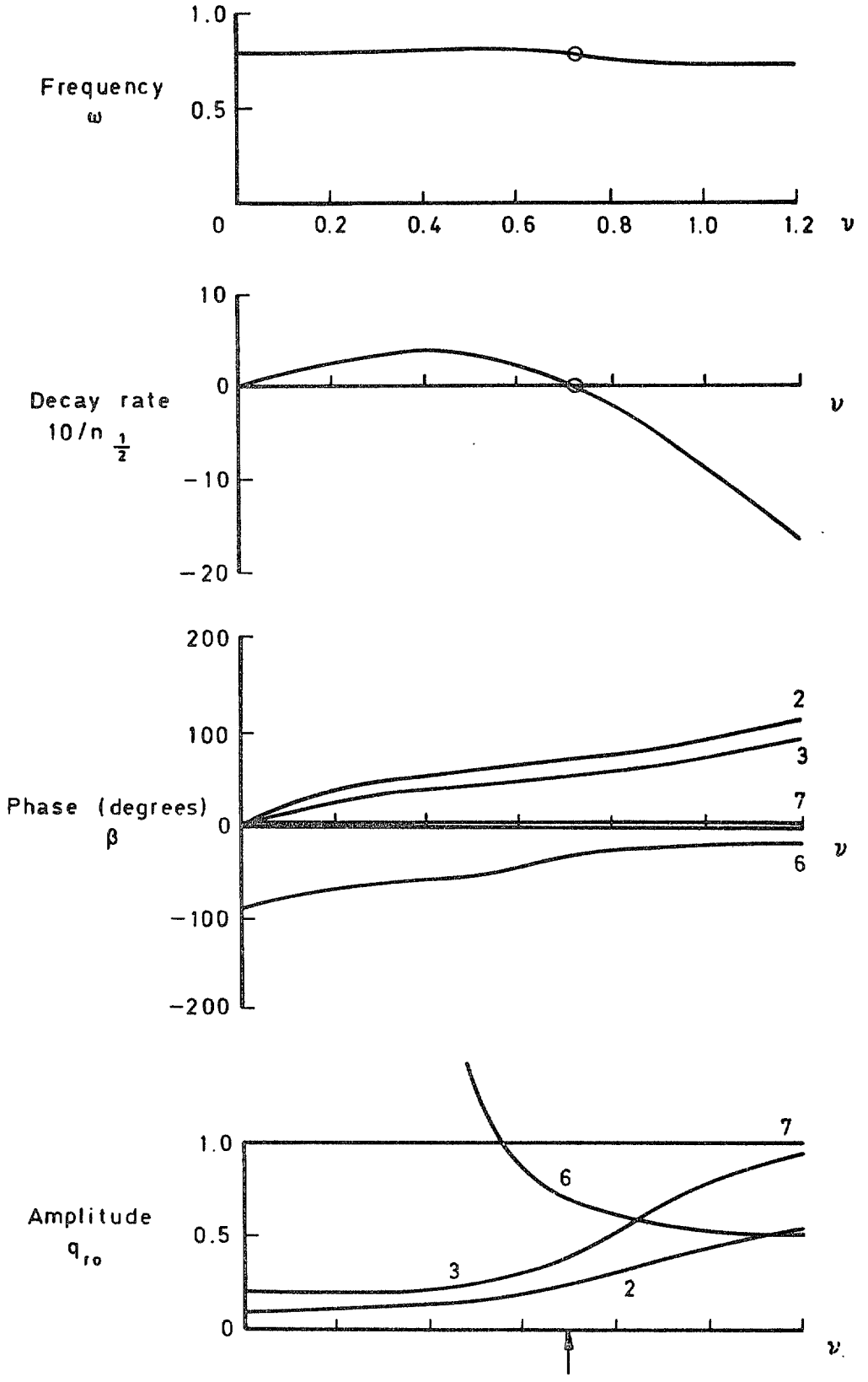

Fig 14 Critical root and eigenvector variation with airspeed — system 2367 — sea level aero damping

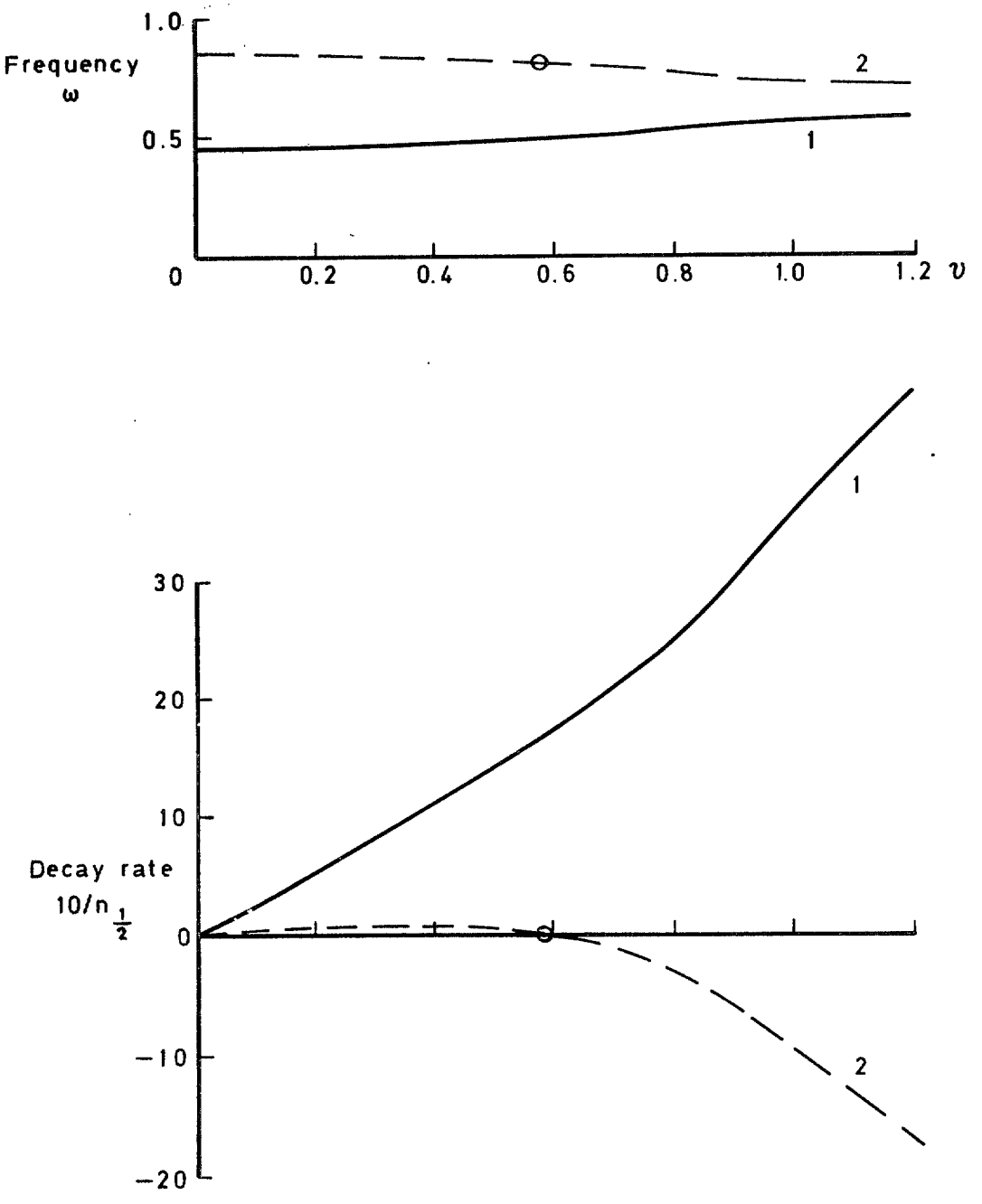

Fig 15 Binary equivalent for flutter type B (2 +3) + (6 + 7)

Fig 16

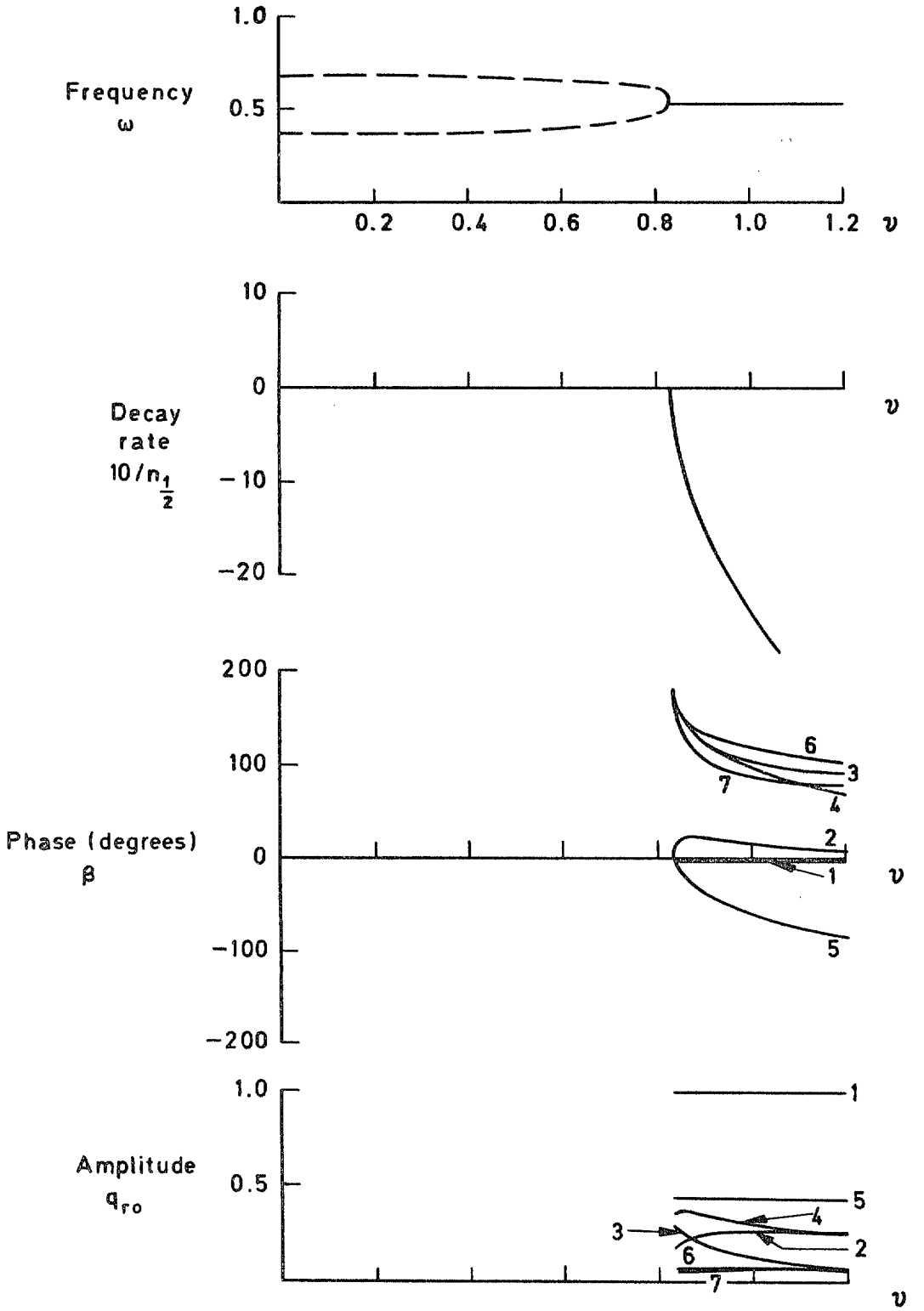

Fig 16 Critical root and eigenvector variation with airspeed — system 1234567 — zero aero damping

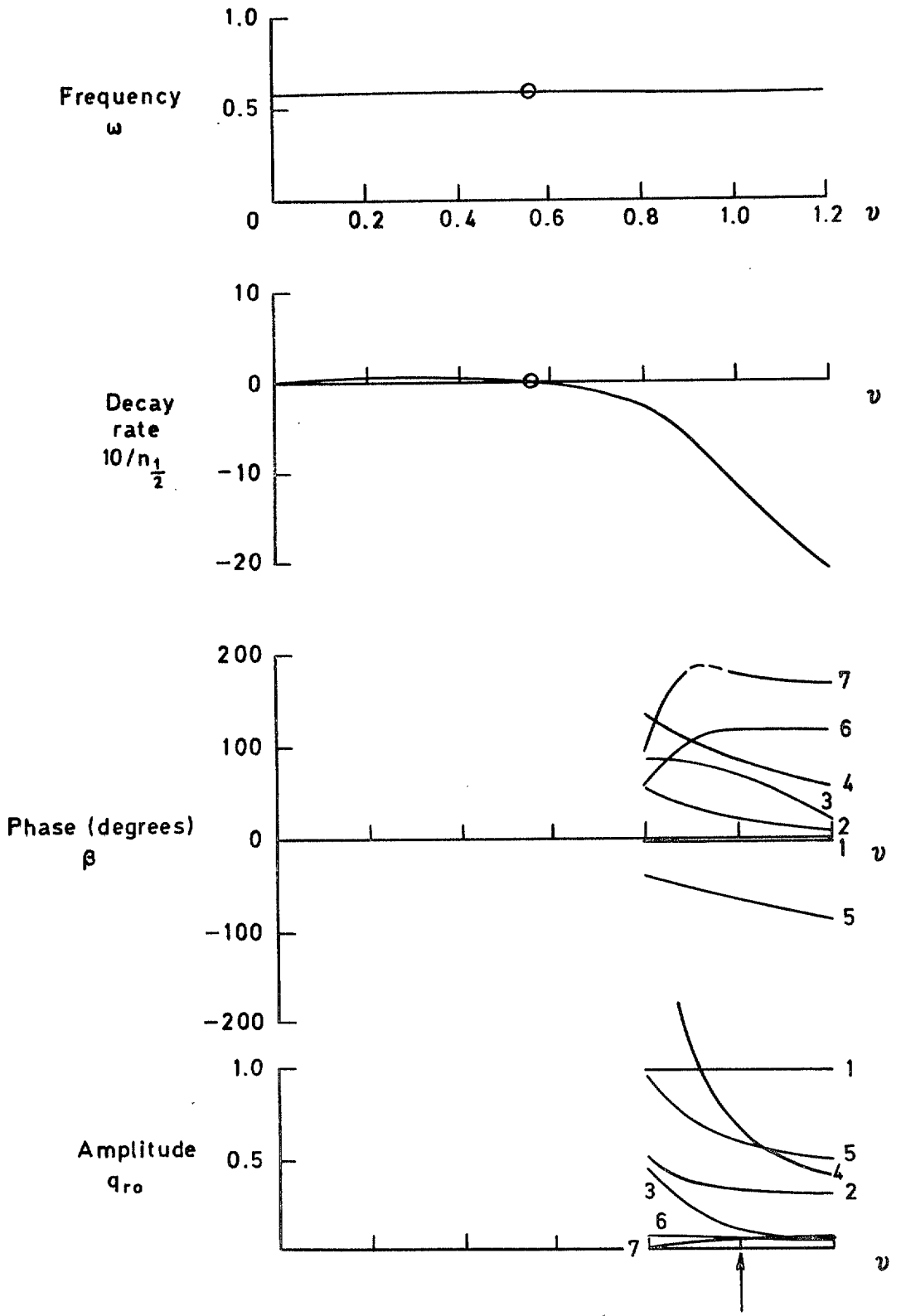

Fig 17 Critical root and eigenvector variation with airspeed — system 1234567 — sea level aero damping

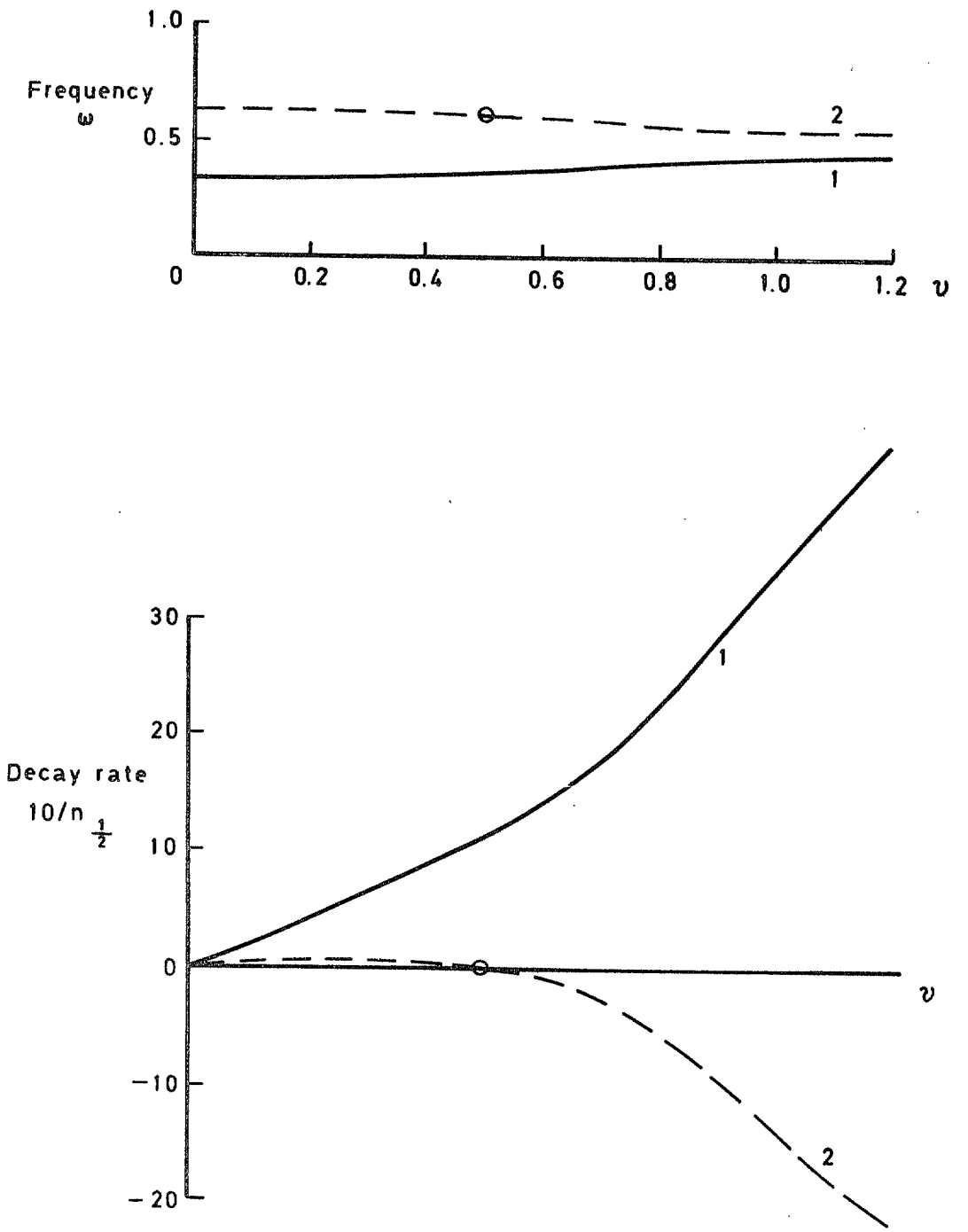

Fig 18 Binary equivalent for flutter type AMS (1 + 2) + (3 + 4 + 5 + 6 + 7)

Printed in England for Her Majesty's Stationery Office by the Royal Aircraft Establishment, Farnborough, Hants. Dd. 586386 K4 2/78.

1979

Published by
HER MAJESTY'S STATIONERY OFFICE

Government Bookshops
49 High Holborn, London WC1V 6HB
13a Castle Street, Edinburgh EH2 3AR
41 The Hayes, Cardiff CF1 1JW
Brazennose Street, Manchester M60 8AS
Southey House, Wine Street, Bristol BS1 2BQ
258 Broad Street, Birmingham B1 2HE
80 Chichester Street, Belfast BT1 4JY

Government Publications are also available through booksellers

R &M No.3832
ISBN 011 471165 8